# Monitoring Chain Dynamics by Luminescence Using a Long-Lived Ruthenium Dye

Cristina Quinn

A thesis
presented to the University of Waterloo
in fulfillment of the
thesis requirement for the degree of
Master of Science
in
Chemistry

Waterloo, Ontario, Canada, 2007

I hereby declare that I am the sole author of this thesis. This is a true copy of the thesis, including any required final revisions, as accepted by my examiners.

I understand that my thesis may be made electronically available to the public.

## ACKNOWLEDGEMENTS

I would like to thank my family for their continual support, encouragement and faith in my abilities. You are all greatly appreciated. I would also like to thank Seb for his help, discussions and friendship.

I am grateful to my supervisor, Professor Jean Duhamel, who provided me with guidance during this difficult journey. I must also express my gratitude to Professor Eric Fillion who spent countless hours helping me with synthesis issues. I am thankful to Jan Venne for her help with the NMR experiments. I would also like to acknowledge Professor Mario Gauthier for his useful comments and suggestions throughout this process.

A special thanks to my lab colleagues Mark Ingratta, Howie Siu, Christine Keyes, Jason Dockendorff and Bushra Siddique for their assistance, support and friendship. You have made this experience unforgettable.

Finally, I would like to thank the University of Waterloo, GWC$^2$, OGSST and NSERC for their financial support.

## ABSTRACT

The purpose of this research project was to determine the feasibility of labelling a water-soluble polymer with a water-soluble dye and quencher. The water-soluble dye chosen was bis-(2,2-bipyridine)-ruthenium(II)-5-amino-1,10-phenanthroline hexafluorophosphate, $RuNH_2$, with a water solubility of $1 \times 10^{-3}$ mol/L. 3,5-Dinitrobenzyl alcohol was found to be an efficient quencher with a quenching rate constant of $2.7 \times 10^9$ $M^{-1} s^{-1}$ as well as a water-solubility of $5 \times 10^{-3}$ mol/L. Both the dye and quencher were modified in a way such that they could be covalently linked to a polymer. $RuNH_2$ was converted to bis-(2,2-bipyridine)-ruthenium(II)-5-isothiocyanato-1,10-phenanthroline hexafluoro-phosphate, RuNCS, using thiophosgene to yield an active isothiocyanate group. 3,5-Dinitrobenzylamine, DNB-$NH_2$, was synthesized via tritylamination of the commercially available 3,5-dinitrobenzyl chloride.

A synthetic pathway has been established to covalently attach the dye and quencher to poly(*N,N*-dimethylacrylamide)(PDMA). Luminescence of this system was first characterized in *N,N*-dimethylformamide (DMF) rather than water to allow for future comparisons to be made between this water-soluble system and the previously established non-water-soluble system. Luminescence analysis of the RuNCS labelled polymers in DMF could be fitted with a sum of three exponentials with the strongest contribution being that of a 1000 ns long-lived species which is characteristic of the free dye. A luminescence decay of a polymer labelled with both RuNCS and DNB-$NH_2$ was acquired and showed static quenching of the ruthenium dye by the quencher.

# Table of Contents

# List of Figures

# List of Schemes

# List of Tables

# Table of Abbreviations

| | |
|---|---|
| AIBN | *a,a'*-azobisisobutyronitrile |
| BOC | *t*-butoxycarbonyl |
| bpy | Bipyridine |
| DMA | *N,N*-Dimethylacrylamide |
| DMF | *N,N*-Dimethylformamide |
| dn/dc | Change in refractive index with change in concentration |
| DNB-Br | 3,5-Dinitrobenzyl Bromide |
| DNB-Cl | 3,5-Dinitrobenzyl Chloride |
| DNB-$NH_2$ | 3,5-Dinitrobenzylamine |
| DNB-OH | 3,5-Dinitrobenzyl alcohol |
| EDA | *N*-BOC-Ethylenediamine |
| ESI-TOF-MS | Electrospray Ionization Time-of-Flight Mass Spectrometry |

| | |
|---|---|
| FBM | Fluorescence Blob Model |
| GC-MS | Gas-Chromatography Mass Spectrometry |
| GPC | Gel Permeation Chromatograhy |
| MLCT | Metal-Ligand Charge Transfer |
| $M_n$ | Number-average molecular weight |
| $M_w$ | Weight-average molecular weight |
| MWCO | Molecular weight cut-off |
| NASI | *N*-Acryloxysuccinimide |
| NMR | Nuclear Magnetic Resonance |
| PDI | Polydispersity index |
| PDMA | Poly(*N*,*N*-dimethylacrylamide) |
| RuNCS | bis-(2,2-bipyridine)-Ruthenium(II)-5-isothiocyanato-1,10-phenanthroline hexafluorophosphate |
| $RuNH_2$ | bis-(2,2-bipyridine)-Ruthenium(II)-5-amino-1,10-phenanthroline hexafluorophosphate |
| TFA | Trifluoroacetic Acid |
| UV | Ultraviolet-Visible Spectrophotometry |

# 1

# Introduction

## 1.1 Polymer Dynamics

Polymer chain dynamics are affected by solvents, temperature, the nature of the backbone, and side chain structure. Several techniques are available for studying polymer chain dynamics such as NMR,[1] light scattering,[2] and molecular dynamics simulations.[3] While these techniques are useful, none lends itself as well as luminescence to obtaining quantitative information on long-range polymer chain dynamics.[4] Luminescence provides information on the dynamics of a single chain, in its entirety, in solution while NMR can only provide information on dynamics occuring over a few bond lengths. Light scattering on the other hand, provides macroscopic information about the dynamic properties of a polymer chain. By using luminescence, experimental quantitative information can be obtained about the dynamics of individual monomers within a polymer.

Long-range polymer chain dynamics refers to the dynamics of encounters between polymeric

units which are far apart from each other. A commonly used chromophore to study long-range chain dynamics by fluorescence is pyrene.[5] When a pyrene molecule absorbs a photon and becomes excited, it can either fluoresce in the blue region ($\sim$ 380 nm) or it can encounter a ground-state pyrene and form an excited dimer known as an excimer. An excimer will either fluoresce in the green region ($\sim$ 480 nm) or dissociate into a ground-state pyrene and an excited state pyrene monomer. Since the formation of an excimer results in quenching of the excited pyrene monomer, pyrene acts as both a chromophore and its quencher. This interesting feature is largely responsible for its popularity as a label for polymer chains since it requires only a single labelling step rather than two when separate dye and quencher molecules are used.

Chain folding dynamics can be probed by monitoring the end-to-end cyclization of a polymer. The use of the process of excimer formation to study end-to-end cyclization was pioneered by Cuniberti and Perico.[6] These experiments involved labelling both ends of a monodisperse chain with pyrene. The intensity of the excimer emission was related to the number of cyclization events which occurred during the lifetime of pyrene. Unfortunately, for pyrene-labelled poly(ethylene oxide), end-to-end cyclization could only be studied for polymers having a maximum molecular weight of 20,000 because the rate of cyclization for polymers larger than 20,000 was too long to be measured within the lifetime of pyrene.[6] This work was later expanded by Winnik et al. who used time-resolved fluorescence to determine quantitatively the rate constant of excimer formation between two pyrenes attached at the ends of a monodisperse polymer.[7] In these experiments, the monomer and excimer fluorescence decays were analyzed with the Birks' scheme given in Scheme 1.1, where $k_1$ and $k_{-1}$ represent the rate constant of excimer formation and dissociation while $\tau_M$

and $\tau_E$ are the monomer and excimer lifetimes, respectively.[8]

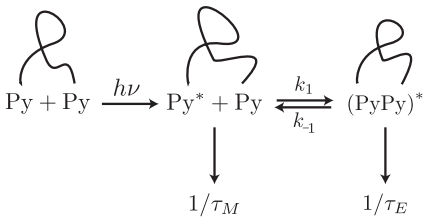


**SCHEME 1.1** Birk's scheme for a pyrene end–labelled polymer chain.

Using end–labelled polymer chains to study long-range polymer chain dynamics has one major drawback in that the bulk of the chain is essentially invisible. For example, with a relatively short polymer containing 100 units, the encounters between only two of these units (the one bearing the quencher and the one bearing the dye) are monitored. In other words, information on the dynamics of the polymer is obtained from only 2% of all monomer units. For end-to-end cyclization studies, this means that only the end units are observed and the middle section is ignored. If one is concerned with the dynamics of the entire polymer chain, this becomes problematic since as the polymer chain increases in length, these two units represent an even smaller fraction of the overall chain. One way to overcome this problem is to randomly label the entire polymer backbone with a dye and its quencher. In this way, the dye may be quenched by any of the quenchers located along the chain rather than only a single specific site such as the ends of the chain. However, random labelling of the polymer chain introduces another complication. Since the rate of encounter depends strongly on the length of chain spanning the dye and its quencher,[8] a distribution of rate constants is obtained for a randomly labelled polymer chain. Scheme 1.2 illustrates the four possi-

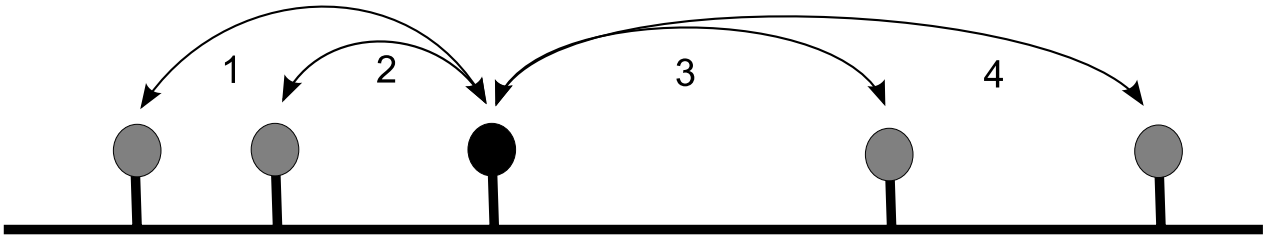


**SCHEME 1.2** Representation of the distribution of rate constants created using a randomly labelled polymer.

ble encounters which can occur for a polymer chain bearing one excited chromophore (black dot) and four quenchers (gray dots). For pyrene, since each chromophore has an equal probability of being excited, the black dot can take any of the other positions so that this particular chain offers $4+3+2+1$=10 different rate constants. It is easy to imagine that as the chain length and amount of labelling increase, a huge number of rate constants are produced. For end-labelled polymer studies, monodisperse polymers are usually used so that a single rate constant describes the cyclization process. However, random labelling of a polymer generates a distribution of rate constants which complicates the analysis of the data since the quenching rate constant is directly proportional to the length of polymer spanning a dye and quencher. The Fluorescence Blob Model (FBM) was introduced by the Duhamel laboratory to circumvent these complications. The FBM allows one to study the dynamics of a randomly labelled polymer chain because it mathematically handles the distribution of rate constants inherent to the random labelling of a chain.[9]

## 1.2 The Fluorescence Blob Model (FBM)

The FBM operates by arbitrarily dividing into blobs the coil of a polymer randomly labelled with pyrene. A blob is defined as the volume probed by an excited chromophore during its lifetime. By dividing the polymer coil into blobs, the FBM shifts the focus of the analysis from the entire polymer chain to a single blob as illustrated in Figure 1.1. Each blob has the same volume, $V_{blob}$, the rate constant of diffusional encounter between a chromophore and a quencher inside a blob is defined as $k_{blob}$ and the rate of exchange of a quencher between blobs is $k_e$. The number of monomer units inside a blob is referred to as $N_{blob}$, the local concentration of blobs inside the polymer coil is defined as $[blob]$, and $\langle n \rangle$ represents the average number of quenchers per blob.

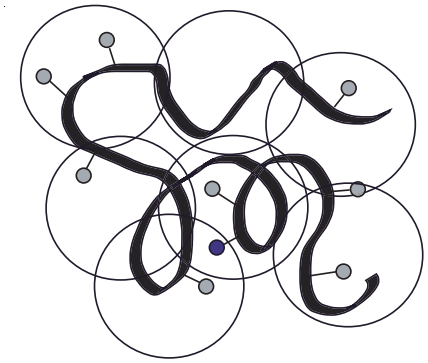

**FIGURE 1.1** Illustration of the Fluorescence Blob Model applied to a polymer chain randomly labelled with a dye (dark circle) and quencher (light circles).

The FBM has so far been applied to several polymeric systems such as polystyrene,[10] poly(*N*,*N*-dimethylacrylamide) (PDMA),[11,12] polypeptides,[13] and hydrophobically modified water-soluble polymers.[5] It has been used to monitor the dynamics of side chains[13] as well as to study the coil-

globule transition of the PDMA backbone.[14] In the present study, the FBM will be applied once more to PDMA. As mentioned previously, pyrene is the most commonly used fluorescent molecule for polymer labelling. The problem with pyrene, however, is that it is extremely hydrophobic. In aqueous solutions, a hydrophobic label will induce the formation of polymer aggregates held together via hydrophobic associations. Therefore, pyrene cannot be used to study the dynamics of a water-soluble polymer in aqueous solution since it would report on polymer aggregates instead of a single chain. This drawback would not be encountered if the polymer was labelled with a water-soluble dye. The goal of this research was to find a water-soluble dye and quencher pair to probe the chain dynamics of a water-soluble polymer in aqueous solution. The polymer of interest was PDMA, a water-soluble polymer, since FBM studies were previously carried out with pyrene-labelled PDMA in acetone and DMF.[11,12] Comparison of the FBM parameters, $k_{blob}$, $k_e[blob]$, and $\langle n \rangle$, for the previously established PDMA system will be made with PDMA labelled with a water-soluble dye and quencher. The second goal of this research, therefore, was to examine the synthetic route required to prepare PDMA labelled with the chosen dye and quencher.

## 1.3 Water–Soluble Dyes

There are several known luminophores which are water–soluble. For the needs of this study, the luminophore must have a sufficiently long lifetime to probe the long-range chain dynamics. For example, the lifetime of the pyrene derivatives used to label polymers are typically on the order of 200 ns. This lifetime allows quenching experiments which reliably probe long-range chain dynamics.

Therefore, a luminophore with a lifetime of at least 200 ns is desired. Most common luminophores such as ethidium bromide and fluorescein have very short lifetimes of a few nanoseconds in aqueous solutions - too short-lived for this study.[15] The popular fluorescein-5-isothiocyanate (FITC) which is often used to label biological macromolecules,[16] has the additional drawbacks of having a significantly reduced quantum yield in acidic solutions and photobleaching within a few minutes at constant illumination.[17]

An interesting group of luminophores which has received a lot of attention in the last 30 years is the ruthenium polypyridine complexes.[18] These complexes have been used as labels for biomolecules[19–22] as well as in light-emitting devices,[23] artificial photosynthetic devices,[24] and oxygen sensors.[25] The broad range of applications for ruthenium bipyridyl complexes is due to their intriguing luminescence properties such as long-lived room temperature luminescence, strong absorption, and thermal stability of the enantiomers with respect to racemization.[18] Ruthenium polypyridine complexes are useful to this study because they are water-soluble and exhibit a long lifetime of about 400 ns at room temperature.[26]

Ruthenium polypyridine complexes are an example of metal-ligand probes. Metal-ligand complexes will be generalized here as a complex formed between a transition metal and one or more diimine ligands. A popular metal-ligand complex is $[Ru(bpy)_3]^{2+}$ where bpy is 2,2'-bipyridine (Figure 1.2). Since this complex contains several aromatic molecules which are hydrophobic, one might be surprised to discover that this complex is water-soluble. This solubility is thought to arise from the two positive charges on the metal. The aromatic ligands are crucial for

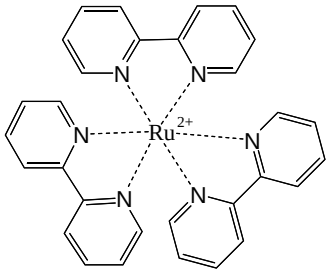


**FIGURE 1.2** Chemical structure of $[\mathrm{Ru(bpy)_3}]^{2+}$.

the absorption and emission of these complexes. The electronic states of the complex which are involved with the luminescence are the $\pi^*$ and d orbitals of the complex, which are associated with the organic ligands and the metal, respectively. Upon absorption of light, an electron is excited from the *d* orbital to the $\pi^*$ orbital. This transition is referred to as a metal-to-ligand charge transfer (MLCT). In the case of $[\mathrm{Ru(bpy)_3}]^{2+}$, ruthenium becomes oxidized and bpy becomes reduced upon absorption of light.

$$[\mathrm{Ru(bpy)_3}]^{2+} + \mathrm{h}\nu \rightarrow [\mathrm{Ru^{III}(bpy)_2(bpy^-)}]^{2+} \tag{1.1}$$

The complex becomes excited to a singlet MLCT state and then undergoes intersystem crossing to the triplet MLCT state as shown in Figure 1.3. The excited state will then decay via radiative or nonradiative pathways. This emission is formally phosphorescence since it arises from a triplet state; however, the excited state is shorter-lived than most phosphorescent states. This is possibly due to spin-orbital coupling with the heavy metal atom.[26] Nevertheless, for $[\mathrm{Ru(bpy)_3}]^{2+}$, the

decay time is still near 400 ns[26] and hence long enough for the needs of this study.

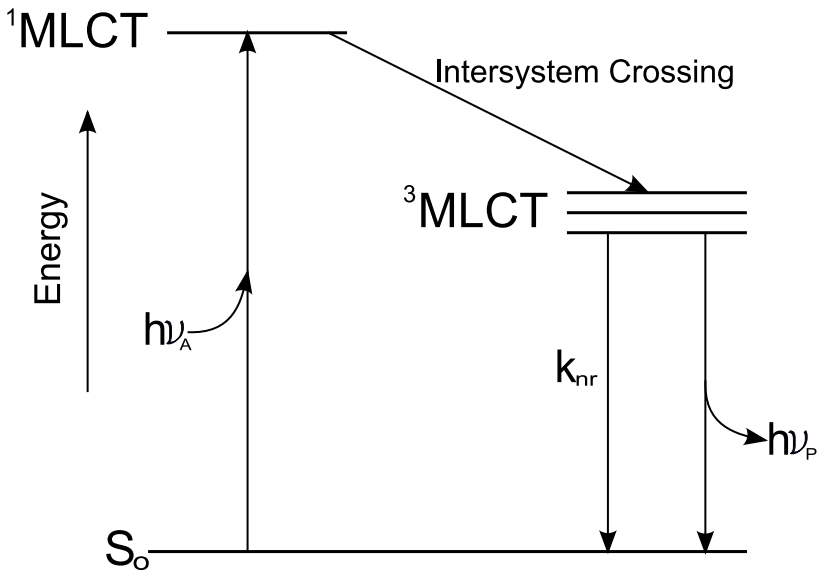


**FIGURE 1.3** Jablonski diagram for a metal-ligand complex.

# 2

# Experimental

## 2.1 Instrumentation

### 2.1.1 Time-Resolved Luminescence Spectroscopy

The time-resolved luminescence decays were obtained using the Time-Correlated Single Photon Counting (TCSPC) technique.[26] Luminescence decays were acquired with the right angle geometry using one of two light sources, either a 5000XeF sub-microsecond xenon flashlamp from IBH Ltd. or a pulsed diode light source from Horiba Jobin Yvon. The pulsed diode light source had a peak wavelength at 463 nm, a maximum repetition rate of 1 MHz and a pulse duration of 1.3 ns. All samples were deoxygenated under a gentle flow of nitrogen gas for 45 minutes prior to acquiring the decay profiles in order to eliminate quenching by oxygen. The excitation wavelength was set to 454 nm in 0.1 M pH 9.6 sodium carbonate aqueous solution or 460 nm in DMF. The emission wavelengths were set to 610 nm, potential light scattering being eliminated by using a

550 nm cut-off filter. The slit-widths were set to 32 nm for both the excitation and emission. All decays were acquired with 20,000 counts at the maximum over 1000 channels.

### 2.1.2 Steady-State Luminescence Measurements

Steady-state luminescence spectra were acquired on a Photon Technology International system with an Ushio 75 XE xenon short arc lamp and an 814 photomultiplier detection system using the right angle geometry. A gentle flow of nitrogen was passed through all samples for 45 minutes prior to acquiring an emission spectrum in order to eliminate oxygen quenching. Emission spectra were obtained by exciting the sample at 454 nm in 0.1 M pH 9.6 sodium carbonate aqueous solution, or 460 nm in DMF. Luminescence intensity of a given sample was obtained by averaging the emission signal from 600-620 nm.

### 2.1.3 Ultraviolet Absorption Measurements

Absorption spectra were obtained with a Hewlett Packard 8452A Diode Array Spectrophotomer. The maximum absorption was limited to a range of 0.1-1.8 using 10 mm quartz cells.

### 2.1.4 Nuclear Magnetic Resonance Spectroscopy (NMR)

All NMR spectra were obtained on a Bruker Avance 300 MHz instrument. The spectrometer was equipped with either a Broadband Observed (bbo) 5 mm probe or a Quadruple Nucleus Probe (qnp) 5 mm probe. The samples were not spun during spectrum acquisition.

### 2.1.5 Gel Permeation Chromatography (GPC)

Gel permeation chromatography was used to characterize the molecular weight of the polymer samples. The instrument comprised a Waters 510 HPLC pump, a Waters 410 differential refractometer detector and a Jordi Gel DVB liner mixed bed column with a length of 500 mm and an internal diameter of 10 mm. The eluent used was DMF at a flow rate of 1 mL/min. A calibration curve was generated with polystyrene standards to obtain apparent (polystyrene-equivalent) molecular weights of the PDMA polymer samples.

### 2.1.6 Light Scattering

The weight-average molecular weight ($\mathrm{M_w}$) of the polymers was determined by Zimm extrapolation to zero angle and zero concentration for a series of 6-8 polymer samples. The polymer sample concentrations ranged from 1.0-8.0 g/L in DMF at angles from 45-145 $^{\circ}$. All samples were filtered through 0.4 $\mu$m PTFE filters prior to measurements. A Brookhaven BI 2030 light scattering goniometer equipped with a Lexel 95 2W argon ion laser (514.5 nm) as the light source was used for the static light scattering measurements. The dn/dc values of the polymers were measured using a Brice-Phoenix differential refractometer equipped with a 510 nm bandpass interference filter.

### 2.1.7 Mass Spectrometry

The mass spectrometry instrument used in this study was equipped with an electrospray ionizer and a quadrupole time-of-flight (QTOF) detector. Positive ion nanoelectrospray (ESI) experiments were carried out on a Waters/Micromass QTOF Ultima Global mass spectrometer. Samples were

infused at a rate of 2 $\mu$L/min in a 1:1 acetonitrile:water mixture. Typical operating conditions consisted of a source temperature of 80 $^{\circ}$C, a capillary voltage of 3.5 kV, a cone voltage of 60-160 V, and a mass resolution of $\sim$9000.

### 2.1.8 Gas Chromatography - Mass Spectrometry (GC-MS)

Low resolution spectra were recorded on an HP G1800A GCD system fitted with a 30 m $\times$ 0.25 mm HP5 column, using an injector temperature of 250 $^{\circ}$C. The temperature program was initially 70 $^{\circ}$C for 2 min a heating rate of 10 $^{\circ}$C/min for 18 min and a final temperature of 250 $^{\circ}$C for 10 min.

## 2.2 Analysis of the Luminescence Decays

The phosphorescence decay curves were fitted by a sum of exponentials (Eq. 2.1) after deconvolution with the lamp decay profile. All fits had a $\chi^2$ = 1.0 $\pm$ 0.1.

$$i_M(t) = \sum_{i=1}^{n_{exp}} a_{M,i} exp(-t/\tau_{M,i}) \qquad n_{exp} = 1, 2, 3 \tag{2.1}$$

## 2.3 Chemicals

All chemicals were used without further purification unless otherwise stated. All reagents were purchased from Sigma-Aldrich unless otherwise stated. All solvents used for synthesis and luminescence experiments were high performance liquid chromatography grade purchased from EMD

Chemicals Inc. (Norwood, OH) unless otherwise stated. Distilled in glass *N,N*-dimethylformamide (DMF) was obtained from Caledon (Georgetown, ON). The ethanol was reagent grade and purchased from Fisher Scientific (Nepean, ON). Dialysis was performed using doubly distilled water (distilled from Millipore Milli-RO 10 Plus and Milli-Q UF Plus (Bedford, MA)).

## 2.4 Synthesis Procedures

### Bis-(2,2-bipyridine)-Ruthenium(II)-5-amino-1,10-phenanthroline hexafluorophosphate ($RuNH_2$)

$Ru(bpy)_2Cl_2$ (0.2 mmol, 100 mg) was dissolved in 5 mL of hot Milli Q water. 5-Amino-1,10-phenanthroline (5-phen) (0.24 mmol, 50 mg) purchased from Polysciences, Inc. (Warrington, PA) was dissolved in 10 mL of hot ethanol. The two solutions were combined and oxygen was removed by bubbling nitrogen gas through the headspace, at room temperature, for 20 min. The reaction was then refluxed for 4 hours. When the reaction was complete, the ethanol was removed by rotary evaporation. Ammonium hexafluorophosphate (1.0 mmol, 162 mg) was added to the solution which was cooled in an ice bath for 20 min. The precipitate was filtered and washed with a minimal amount of Milli Q water ($2 \times 0.5$ mL). The precipitate was dried under vacuum for 1 hour and then redissolved in a minimal amount of acetone ($\sim$1 mL) and purified using a neutral alumina column of $\sim$5 cm in height and 1.5 cm in diameter. The product was retrieved from the column using a 1:2 toluene:acetonitrile mixture as the eluent. The fractions were collected and dried under vacuum. The product was further purified by recrystallization from a minimal amount

of acetone into cold stirring ether. The precipitate was dried under vacuum and a yield of 156 mg or 87% was obtained. $^1$H NMR (300 MHz, $CD_3CN$): $\delta$ = 8.60-7.15 (m, 23 H, aromatic), 5.54 (s, 2 H, $NH_2$).

*Chromatography Note:* The literature reports the use of a 2:1 toluene:acetonitrile mixture as the solvent used for column chromatography. However, thin layer chromatography showed that, for this solvent system, the unreacted 5-phen had the same $R_f$ value as the desired product while unreacted $Ru(bpy)_2Cl_2$ remained at the baseline. Although 5-Phen is insoluble in acetone and therefore can be filtered out prior to introduction on the column, a more appropriate solvent mixture is 1:2 toluene:acetonitrile. This mixture allows the desired complex to have a much larger $R_f$ than 5-phen while $Ru(bpy)_2Cl_2$ remains at the baseline. Also note that the $R_f$ of compounds on the TLC plate is usually not 100% representative of the column $R_f$ despite the fact that the same solvent and matrix systems are being used. The reason for this is yet to be understood.

### Bis-(2,2-bipyridine)-Ru(II)-5-isothiocyanato-1,10-phenanthroline hexafluorophosphate (RuNCS)

$RuNH_2$ (0.11 mmol, 76 mg) was added to a mixture of Milli Q water (10 mL) and Amberlite IRA-400(Cl) ion exchange resin and stirred for 1.5 hours in order to exchange the hexafluorophosphate counterions for chlorine ions, making the ruthenium compound more soluble in water. The solution was filtered to remove the resin which was washed twice with Milli Q water ($2 \times 7$ mL). The aqueous solution was concentrated and oxygen was removed from the vessel by flushing it with nitrogen gas. Thiophosgene (0.13 mmol, 11 $\mu$L) in 5 mL of acetone was added dropwise to

the aqueous solution over 30 min while the reaction vessel was kept on ice. The solution was stirred at room temperature for 12 hours in the dark. The product was recovered by concentrating the solution and adding $NH_4PF_6$ to the solution. $NH_4PF_6$ was added in excess to allow the hexafluorophosphate ions to displace chlorine as the counterion allowing the ruthenium product to precipitate. The product was isolated by filtration and dried under vacuum. The crude yield was 97%. By $^1$H NMR (see Figure A.3 in Appendix A), the amine protons are no longer present and therefore must have reacted. The aromatic region of the spectrum has a different coupling pattern but it is still difficult to distinguish individual proton signals. By ESI-TOF-MS (see Figure A.4 in Appendix A), the final product was found to be a mixture of $RuNH_2$, RuNCS, and a ruthenium dimer formed by the reaction between RuNCS and $RuNH_2$. The formation of the dimer might be suppressed by adding the ruthenium mixture to the thiophosgene solution in acetone rather than the other way around. However, due to the reactivity of thiophosgene with water, it is safer to add the thiophosgene/acetone solution to the aqueous solution as was done in this thesis. Also, by adding $NaHCO_3$ to the mixture, the reaction would proceed further since a base is required to scavenge the amine protons. Purification of the products was not possible by chromatography, recrystallization or liquid-liquid extraction due to the similarity of the compounds. Since $RuNH_2$ and its dimer are both unreactive towards further coupling reactions, the mixture was used without further purification. Thiophosgene was only handled in the fumehood due to its toxicity. $^1$H NMR (300 MHz, $CD_3CN$): $\delta$ = 8.75-7.25 (m, 23 H, aromatic).

### 3,5-Dinitrobenzaldehyde (DNB=O)

Ytterbium(III) triflate ($Yb(OTf)_3$) (0.25 mmol, 175 mg) and $HNO_3$ (2.5 mmol, 0.11 mL) were added to a solution of 3,5-dinitrobenzyl alcohol (2.52 mmol, 0.50 g) in dichloroethane (5 mL). The solution was flushed with nitrogen and then refluxed at approximately 110 $^{\circ}C$ for 24 hrs. Upon completion, the reaction mixture was cooled to room temperature. Water (10 mL) was added and the aldehyde was extracted into dichloromethane ($2 \times 10$ mL). The organic fractions were combined and dried with $MgSO_4$ and concentrated. Using a silica column and dichloromethane as the eluent, the desired aldehyde was purified and isolated in a 20% yield. $^1$H NMR (300 MHz, $CDCl_3$): $\delta$ = 10.23 (s, 1 H, CHO), 9.31 (t, 1 H, *J*=2.04 Hz, CH), 9.06 (d, 2H, *J*=2.04 Hz, CH).

### 3,5-Dinitrobenzylamine (a) (DNB-$NH_2$)

3,5-Dinitrobenzyl aldehyde (0.26 mmol, 50 mg) and ammonium acetate (2.6 mmol, 200 mg) were added to methanol (5 mL). The solution was stirred at room temperature for 2 hours followed by the addition of $NaCNBH_3$ (0.18 mmol, 11 mg) and 3Å molecular sieves (50 mg). The mixture was stirred at room temperature for an additional 36 hours. Concentrated HCl was added to the solution until pH$<$2 in order to form the amine salt. Ether was added to the mixture and a precipitate formed. The precipitate was filtered, redissolved in water, basified to pH$>$10 with KOH and saturated with NaCl. The product was extracted with dichloromethane ($4 \times 10$ mL), dried over $MgSO_4$, and concentrated. The product was further purified by recrystallization from dichloromethane/ether. By GC-MS, the product appeared to be a mixture of DNB-OH and DNB-$NH_2$. Precipitation and filtering of the amine was complicated by the fineness of the precipitate,

preventing a final pure product from being obtained. $^{1}$H NMR (300 MHz, $CDCl_3$): $\delta$ = 8.99 (s, 1, CH), 8.53 (s, 2H, CH), 8.53 (d, 2H, CH), 5.27 (s, 2H, $CH_2$).

### 3,5-Dinitrobenzyl bromide (DNB-Br)

Triphenylphosphine (3.03 mmol, 0.8 g) and imidazole (3.03 mmol, 0.26 g) were added to 10 mL of dry dichloromethane and stirred for 5 min. Bromine (3.03 mmol, 0.15 mL) was added dropwise to the solution and the mixture was stirred at room temperature for another 5 min. 3,5-Dinitrobenzyl alcohol (2.52 mmol, 0.5 g) was added to the mixture and the reaction flask was flushed with nitrogen. The reaction was stirred for an additional 45 min. at room temperature. The imidazole salt was removed from the solution by filtration and the eluent concentrated and purified by column chromatography using silica and ethyl acetate. A yield of 79% for the purified product was obtained. $^{1}$H NMR (300 MHz, $CDCl_3$): $\delta$ = 8.97 (s, 1 H, CH), 8.57 (s, 2H, CH), 4.59 (s, 2H, $CH_2$).

### (3,5-Dinitrobenzyl)-tritylamine

To a mixture of acetonitrile (10 mL) and acetone (3 mL) was added 3,5-dinitrobenzyl chloride (or bromide) (2.3 mmol, 0.5 g) and tritylamine (4.6 mmol, 1.2 g). The mixture was stirred in the dark at room temperature for 2 days. When the reaction was complete, the solvents were evaporated and the residue was redissolved in acetonitrile. The tritylamine salt was removed from the solution by filtration and the eluent containing the desired product was concentrated and dried under vacuum. The product was further purified by removing the tritylamine salt through recrystallization from

ethanol. The supernatants of several recrystallizations were combined and dried to give a 70% yield of the desired 3,5-dinitrobenzyl-tritylamine. $^1$H NMR (300 MHz, $CDCl_3$): $\delta$ = 9.00 (t, 1 H, *J*=1.95 Hz, CH), 8.59 (s, 2H, *J*=1.88 Hz, CH), 7.23 (m, 15H, $C_6H_5$), 4.74 (s, 2H, $CH_2$).

### 3,5-Dinitrobenzylamine hydrochloride(b) (DNB-$NH_2$)

(3,5-Dinitrobenzyl)-tritylamine (1.1 mmol, 0.480 g) was dissolved in 5 mL trifluoroacetic acid (TFA)/dichloromethane (60/40 v/v). The solution immediately turned dark yellow and was stirred at room temperature. After 2 hours, methanol (3 mL) was added to the solution causing the solution to immediately turn clear. The mixture was stirred at room temperature for another 2 hours. The solvents were then evaporated under reduced pressure and the product was dried under vacuum at room temperature to further remove TFA. The product was precipitated from methanol into hexanes to give a final purified yield of 86%. $^1$H NMR (300 MHz, DMSO): $\delta$ = 8.77 (t, 1 H, *J*=1.99 Hz, CH), 8.75 (d, 1 H, *J*=1.88 Hz, CH), 7.29 (s, 1 H, $NH_3$, exchangeable with $D_2O$), 7.12 (s, 1 H, $NH_3$, exchangeable with $D_2O$), 6.95 (s, 1 H, $NH_3$, exchangeable with $D_2O$).

### *N*-Acryloxysuccinimide (NASI)

Acrylic acid (70 mmol, 5.00 g) and *N*-hydroxysuccinimide (58 mmol, 6.66 g) were added to dichloromethane (200 mL) and cooled to -5 °C. To the cold solution was added 1,3-dicyclohexyl-carbodiimide (DCC) (58 mmol, 11.9 g). The mixture was stirred at -5 °C for 5 hours and then at 5 °C overnight. The dicyclohexylurea (DCU) biproduct was removed by filtration. The eluent was concentrated and extracted against 5% $NaHCO_3$ ($3\times$ 75 mL) and 0.3 N HCl ($2\times 50$ mL). The

dichloromethane fractions were dried with $MgSO_4$, the solvent was removed by rotary evaporation and the product was redissolved in ethyl acetate. Remaining dicyclohexyl urea was removed by filtration. The eluent was concentrated and precipitated in hexane. The product was recrystallized in isopropyl alcohol to yield the purified product, as evidenced by $^1$H NMR. The purified yield was 32%. $^1$H NMR (300 MHz, $CDCl_3$): $\delta$ = 6.72 (d, 1 H, *J*=17.2 Hz, $H_2C$=C), 6.3 (m, 1H, HC=C), 6.13 (d, 1H, *J*=7.8 Hz, $H_2C$=C), 2.85 (s, 4H, $CH_2$).

### NASI/DMA Copolymer

Random copolymerization was carried out using AIBN which was recrystallized twice from ethanol. In a typical reaction NASI (0.964 mmol, 0.163 g), distilled *N*,*N*-dimethylacrylamide (23 mmol, 2.4 mL), and AIBN (60 $\mu$mol, 10 mg) were combined in DMF (12 mL) and added to a Schlenk tube. The solution was deaerated by bubbling nitrogen through the solution for 10 minutes, then sealed and heated at 50 $^{\circ}$C. The polymerization reaction was quenched by putting the flask in ice once the reaction had reached 10-20 % conversion (as determined by the NMR spectra). Conversion in this range was required to control monomer composition (see Section 4.2.1). The polymer was then purified by precipitation, once from DMF to diethyl ether and once from acetone to diethyl ether. The molecular weights of several polymers were measured. PDMA was synthesized and found to have $M_w$ = 900 000 g/mol by light scattering. By GPC, a DMA/NASI copolymer had an apparent $M_n$ = 400 000 relative to polystyrene standards and a PDI of 1.24.

### Labelling the NASI/DMA Copolymer

In a typical reaction, the NASI/DMA copolymer (170 mg) was dissolved in DMF (5 mL). *N*-BOC-Ethylenediamine (9.3 $\mu$mol, 1.5 $\mu$L) and triethylamine (23 $\mu$mol, 3.1 $\mu$L) were added to the mixture and the solution was stirred in the dark at room temperature. After 24 hours, DNB-$NH_2$ (42 $\mu$mol, 10 mg) was added along with additional triethylamine (126 $\mu$mol, 17 $\mu$L). The mixture was stirred another 48 hours at room temperature and then dialyzed extensively (MWCO = 2000). The polymer was recovered by freeze drying to yield 62 mg. Deprotection of the BOC group was accomplished by dissolving the polymer in TFA (1.5 mL) and stirring at room temperature for 1.5 hours. TFA was removed by rotary evaporation followed by precipitation of the amine salt of the polymer from acetone into hexane twice. The polymer was dried under vacuum for one hour and then redissolved in DMF. RuNCS (10 mg) was added to the solution, left at 5 $^{o}$C overnight, in the dark, with minimal agitation. Dialysis (MWCO = 2000) of the mixture followed by freeze drying yielded the fully labelled polymer. A final yield of 59 mg was obtained.

# 3

# Selection of Dye and Quencher

## 3.1 Introduction

A luminophore requires several charateristics in order to be suitable for this study. It must have a lifetime of at least 200 ns, its structure must allow for its covalent attachment to the polymer chain, and it must be water-soluble. Based on these criteria, bis-(2,2'-bipyridine)-ruthenium(II)-5-amino-1,10-phenanthroline hexafluorophosphate ($RuNH_2$) (Figure 3.1a) was selected. Ruthenium bipyridine complexes have a lifetime of $\sim$400 ns.[26] The amine group on the phenanthroline ligand allows the covalent attachment of the dye to a polymer chain and the positive charge on the ruthenium promotes solubility in water. This dye has been previously synthesized by the Ellis group[27] and was used to label poly(L-lysine).[28] The selected quencher is 3,5-dinitrobenzyl alcohol (DNB-OH) (Figure 3.1b). This quencher was selected based on its structural resemblance to 3,5-

dinitrotoluene, a known efficient quencher for [Ru(bpy)$_3$].[29] The polarity of the nitro and alcohol groups are expected to increase the water solubility of DNB-OH.

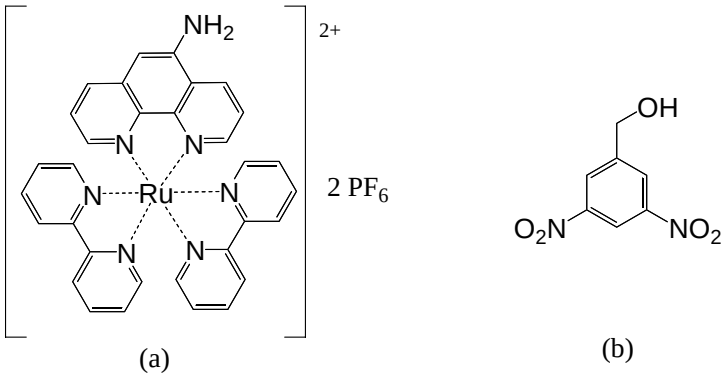


(a) (b)

**FIGURE 3.1** a) Structure of the dye, RuNH$_2$; b) Structure of the quencher, DNB-OH.

## 3.2 Results and Discussion

### 3.2.1 Bis-(2,2'-bipyridine)-ruthenium(II)-5-amino-1,10-phenanthroline hexafluorophosphate

The dye was successfully synthesized according to Scheme 3.1 by coupling 5-amino-1,10-phenanthroline with *cis*-bis(2,2'-bipyridine)dichlororuthenium(II) hydrate (Ru(bpy)$_2$Cl$_2$). The structure of the final product was verified by $^1$H NMR spectroscopy as well as by ESI-TOF-MS. These spectra are shown in Figures A.1 and A.2 in Appendix A.

The photophysical properties of the dye were examined by UV-Vis absorption and luminescence and compared to reported literature values. Upon excitation of the dye at 454 nm, an emis-

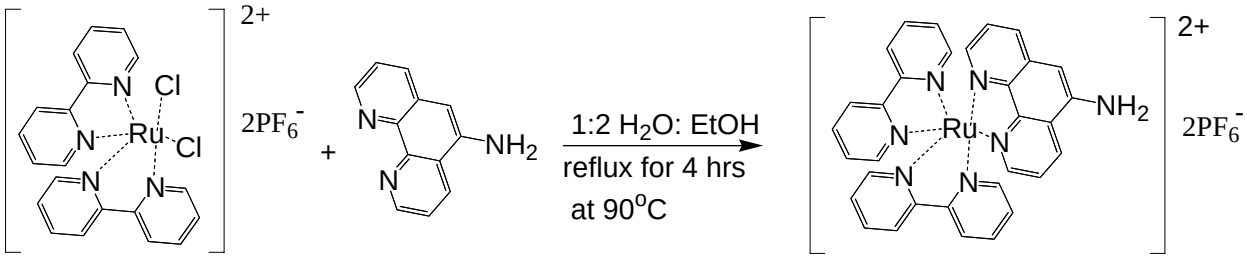


**SCHEME 3.1** Synthesis of $RuNH_2$

sion at 610 nm was observed in a 0.1 M $Na_2CO_3$ aqueous solution at pH 9.6 (Figure 3.2). The extinction coefficient of the $RuNH_2$ dye in 0.1 M $Na_2CO_3$ aqueous solution at pH 9.6 was found to equal 13,700 $\pm$ 100 $M^{-1}cm^{-1}$ at 454 nm. The extinction coefficient is in agreement with the reported value of 13,800 $M^{-1}cm^{-1}$ at 454 nm.[28] The extinction coefficient value was obtained by preparing several solutions of a known concentration of $RuNH_2$ and measuring their absorbtion. From the Beer-Lambert law given in Equation 3.1, the slope of a plot of absorbance versus concentration equals the extinction coefficient ($\epsilon$) of that species, at a specific wavelength, times the pathlength (L) of the absorption cuvette, which is usually equal to 1 cm.

$$Absorbance = \epsilon[Dye]L \tag{3.1}$$

The luminescence decay of $RuNH_2$ was acquired by the single-photon counting technique. The $RuNH_2$ decay was biexponential, as shown in Figure 3.3, and was fit with a $\chi^2$ of 1.02. The lifetimes were 570 $\pm$45 ns and 3600 $\pm$340 ns in deaerated 0.1 M $Na_2CO_3$ aqueous solution

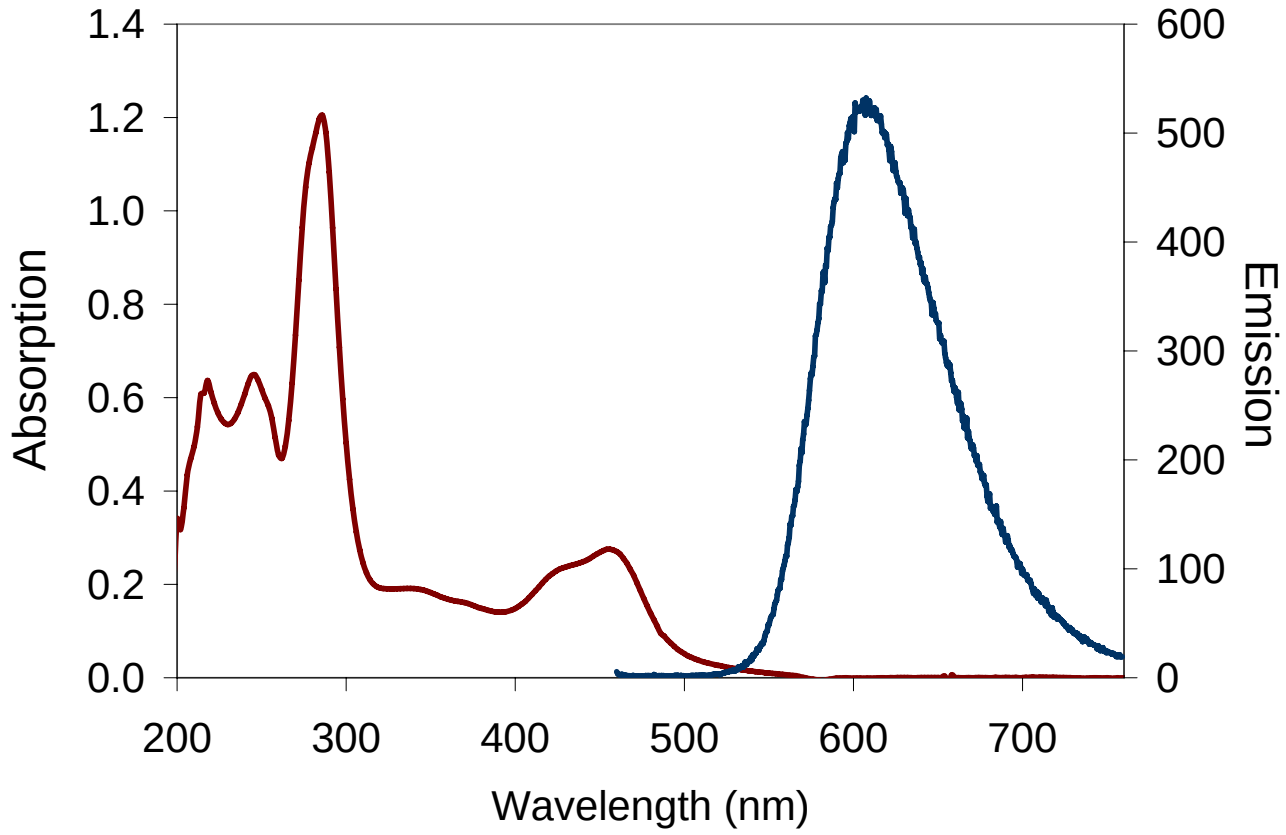


**FIGURE 3.2** Absorption and emission spectrum of $RuNH_2$ in deaerated 0.1 M $Na_2CO_3$ aqueous solution at pH 9.6.

at pH 9.6 with pre-exponential factors of 0.98 $\pm$0.02 and 0.02 $\pm$0.02, respectively. This decay was obtained with a Xenon flashlamp which exhibits a broad emission pulse. Because of this broad pulse, all decays acquired on the instrument exhibit a long lifetime. Therefore, the second long-lived lifetime of 3600 ns observed for $RuNH_2$ is an artifact of the lamp rather than a real lifetime. The lifetime of $RuNH_2$ in a 0.1 M $Na_2CO_3$ aqueous solution at pH 9.6 has been reported to equal 639 ns.[28] Since the structure of the dye synthesized in this project has been confirmed by both $^1H$ NMR and mass spectrometry, and the extinction coefficient at 454 nm is equal to

the reported literature value, the difference in luminescence lifetime must be due to a difference in the experimental conditions used to acquire the luminescence decays. Possible differences in experimental conditions include unknown impurities in the solution, differences in the degassing technique, method of decay analysis, as well as instrumentation resolution.

The second requirement for the dye was that it be covalently attached to the polymer backbone. Several coupling reactions, directed at the amine substituent of this dye, were attempted. However, the amine substituent on the phenanthroline never reacted with acetyl chloride nor activated acrylic acid – presumably due to a weakening of the electron-donating ability of the amine substituent on the phenanthroline ligand by the aromatic groups. For this reason, the amine substituent was converted to an isothiocyanate group using thiophosgene to ultimately attach the dye to the polymer via a covalent thiourea linkage. The procedure for this modification closely followed that reported by Ryan et al.[28] Scheme 3.2 illustrates the synthesis of the isocyanate derivative, RuNCS.

The final requirement for the luminophore is that it be water-soluble. The solubility of pyrene in water is $6.8 \times 10^{-7}$ mol/L.[30] Since $RuNH_2$ contains three highly aromatic ligands, it would be expected that it would also be weakly soluble in water. However, it has a solubility of $\sim 1 \times 10^{-3}$ mol/L in 0.1 M $Na_2CO_3$ aqueous solution at pH 9.6, a solubility approximately three orders of magnitude larger than that of pyrene. It is thought that this increased solubility is due to the two positive charges on the ruthenium atom. Since $RuNH_2$ is 1000 times more soluble in water than pyrene, no aggregation is expected to occur at the concentrations required for the luminescence

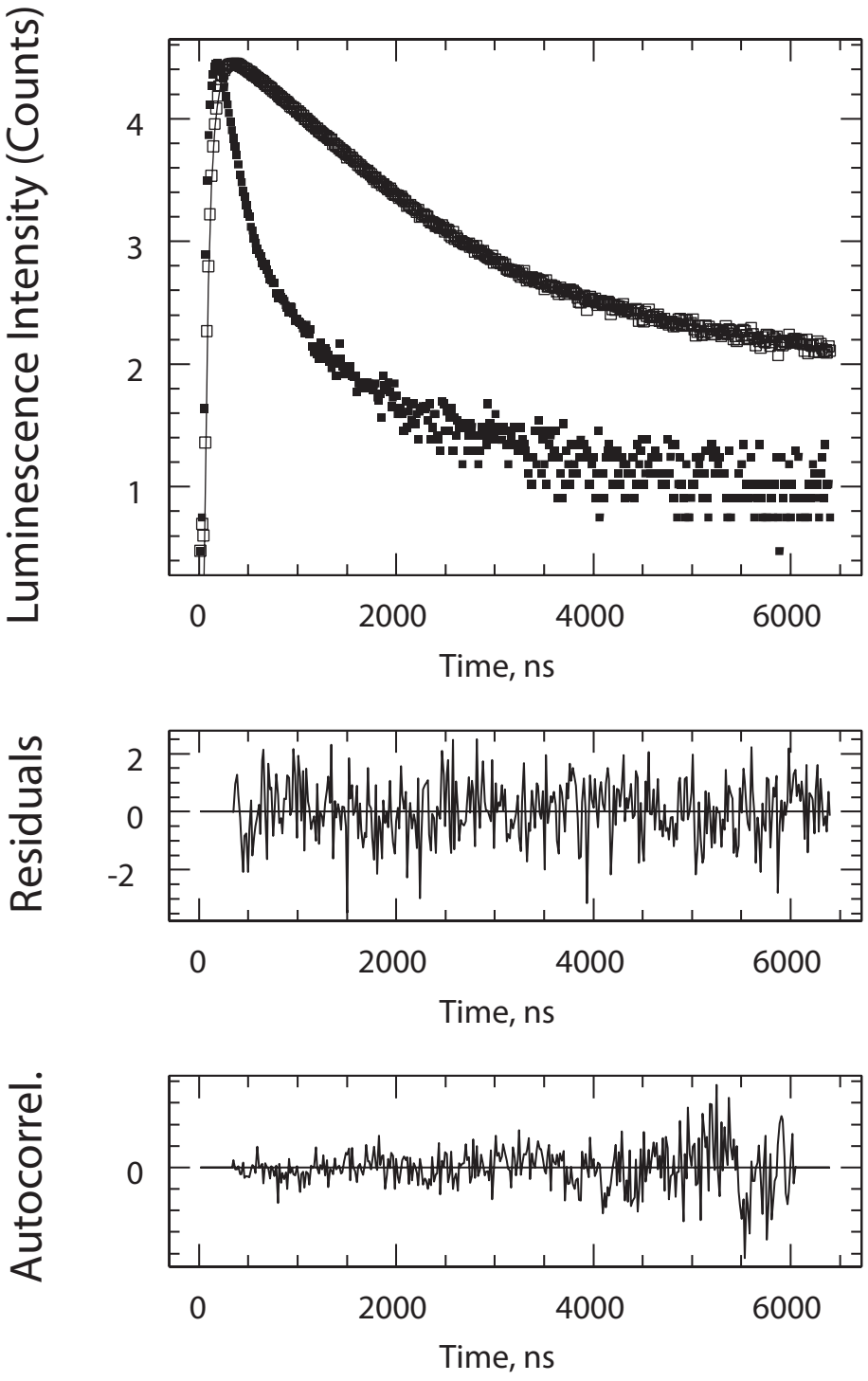


**FIGURE 3.3** Luminescence decay of $RuNH_2$ in deaerated 0.1 M $Na_2CO_3$ aqueous solution at pH 9.6 using the Xe flashlamp. $\lambda_{ex} = 454$ nm, $\lambda_{em} = 610$ nm, [$RuNH_2$] = 7 $\mu$M, and time per channel of 16 ns.

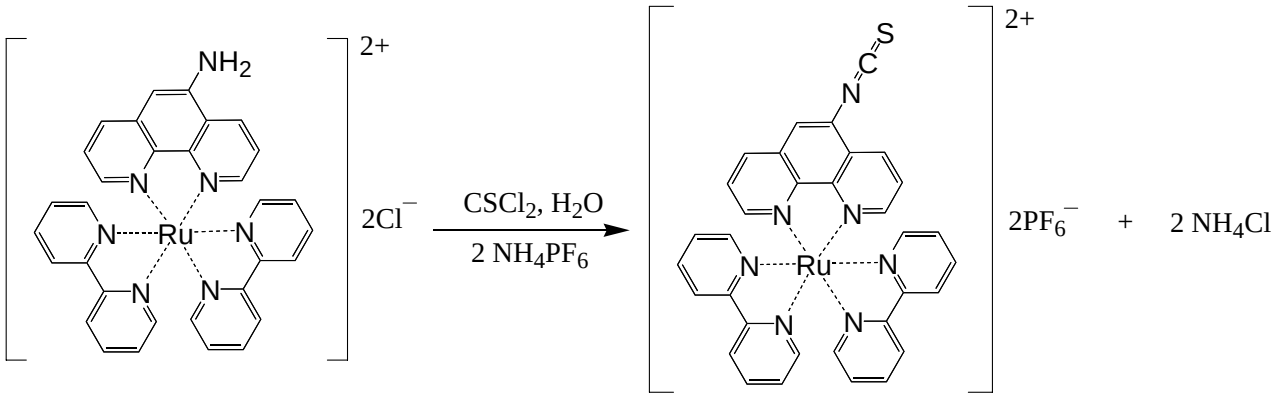


**SCHEME 3.2** Synthesis of RuNCS

experiments.

Although the final goal of this research was to analyze the water-soluble polymer PDMA in water, the behaviour of the labelled polymer must first be investigated in DMF. Since pyrene-labelled PDMA in DMF has already been studied according to the FBM, comparisons between the two labelled polymers must be made. For this reason, the luminescence of $RuNH_2$ in DMF was also measured (Figure 3.4). This decay was acquired using NanoLED excitation ($\lambda_{ex}$ = 460 nm, $\lambda_{em}$ = 610 nm) at 100 kHz. The monoexponential decay was well-fitted with a $\chi^2$ of 1.02 and a lifetime of 965 ns using a time per channel of 10.08 ns. This lifetime is significantly longer than that observed in water. Such an effect is usually due to a larger non-radiative rate constant as seen from Eq. 3.2 where $k_r$ and $k_{nr}$ are the radiative and non-radiative rate constants, respectively.[31]

$$\tau = \frac{1}{k_r + k_{nr}} \tag{3.2}$$

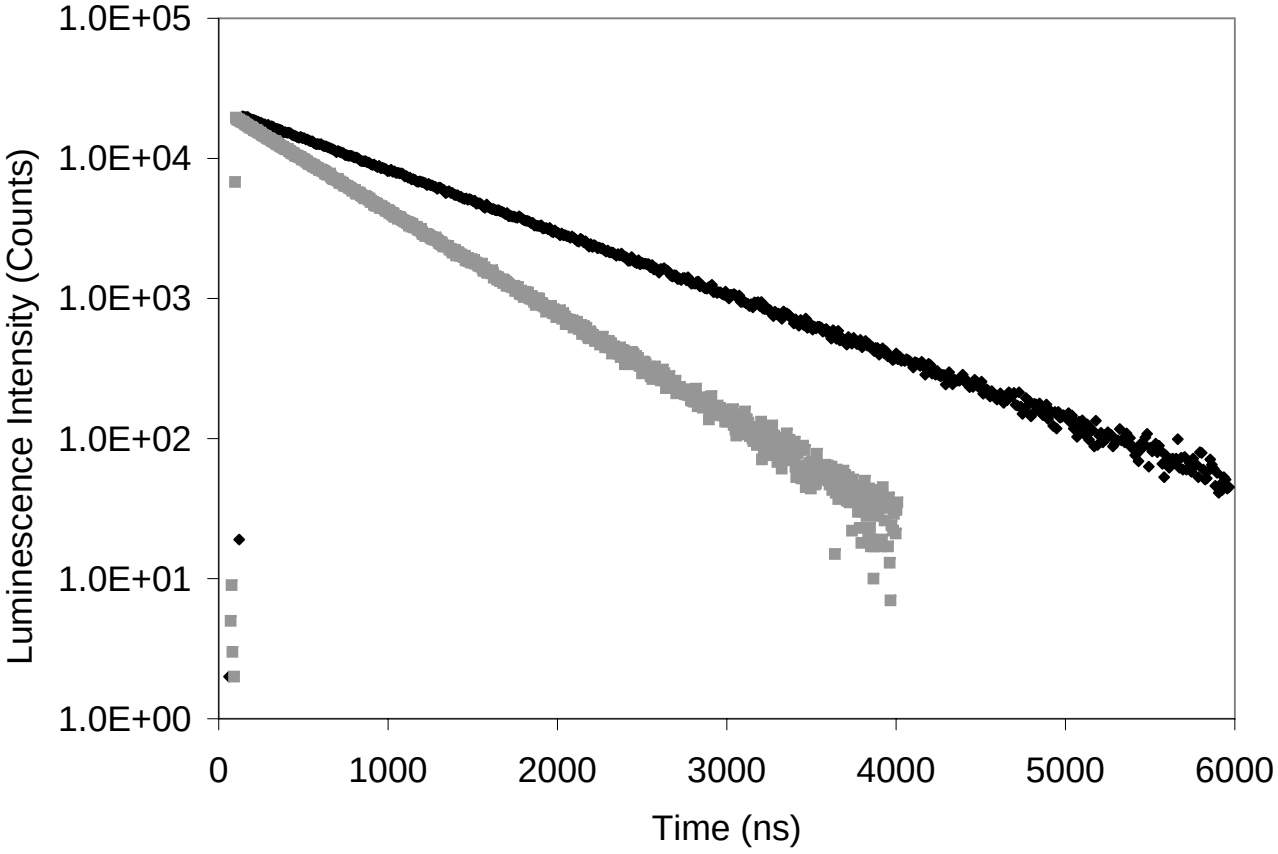


**FIGURE 3.4** Lifetime decays of $RuNH_2$ (10 $\mu$M) in DMF with quencher ([DNB-OH] = 0.2 $\mu$M) (grey line) and without quencher (black line). The lifetimes are 600 and 965 ns, respectively.

### 3.2.2 3,5-Dinitrobenzyl alcohol

The selection of the luminescence quencher followed three main criteria. First, the excited $RuNH_2$ must be quenched by collisional encounters, second, the quencher must be water-soluble, and

finally, it must allow for covalent attachment onto the polymer. Several molecules were investigated to use as a quencher of $RuNH_2$ including triethylamine, *N,N*-dimethylethanolamine, nitromethane, and iodomethane. The strongest collisional quencher was found to be 3,5-dinitrobenzyl alcohol (DNB-OH). The quenching of $RuNH_2$ by DNB-OH is illustrated in Figure 3.5.

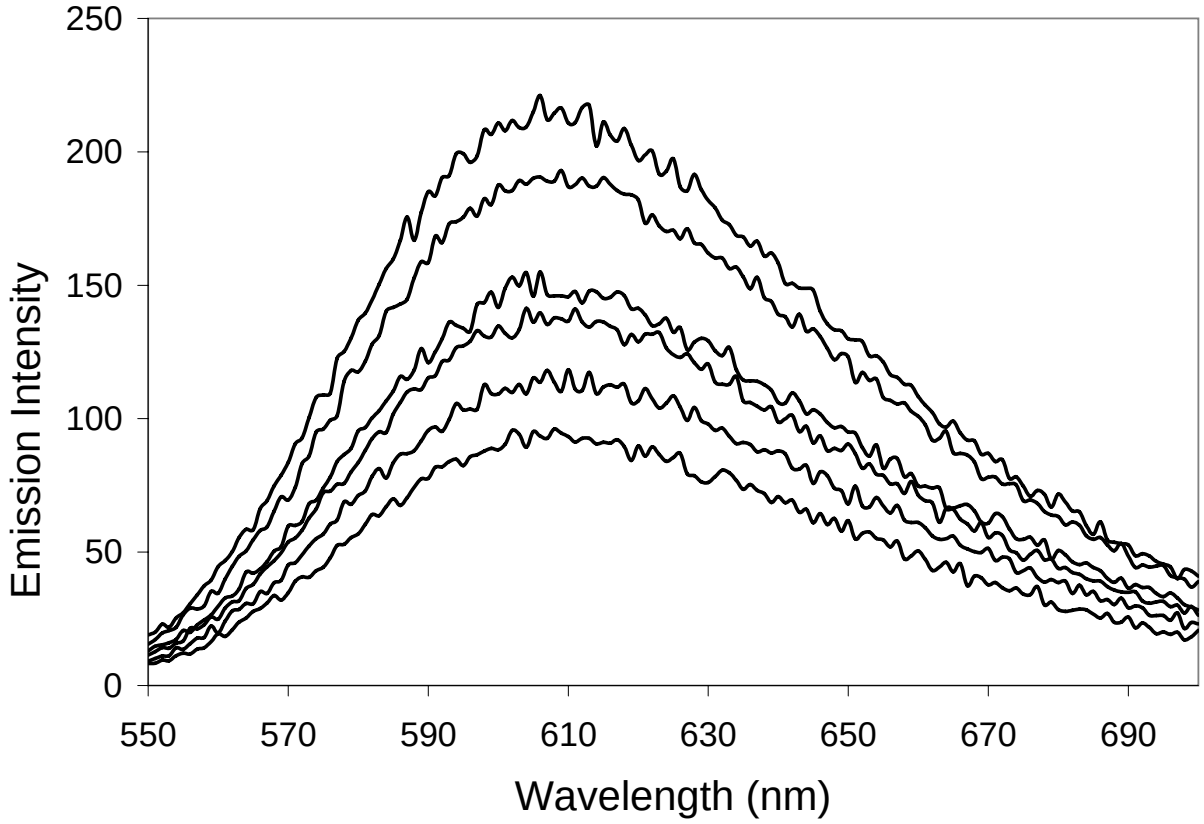


**FIGURE 3.5** Quenching of the $RuNH_2$ luminescence by DNB-OH in deaerated 0.1 M $Na_2CO_3$ aqueous solution at pH 9.6. The DNB-OH concentration is varied from 0 $\mu$M (top) to 50 $\mu$M (bottom). $\lambda_{ex} = 454$ nm, $[RuNH_2] = 47\ \mu$M.

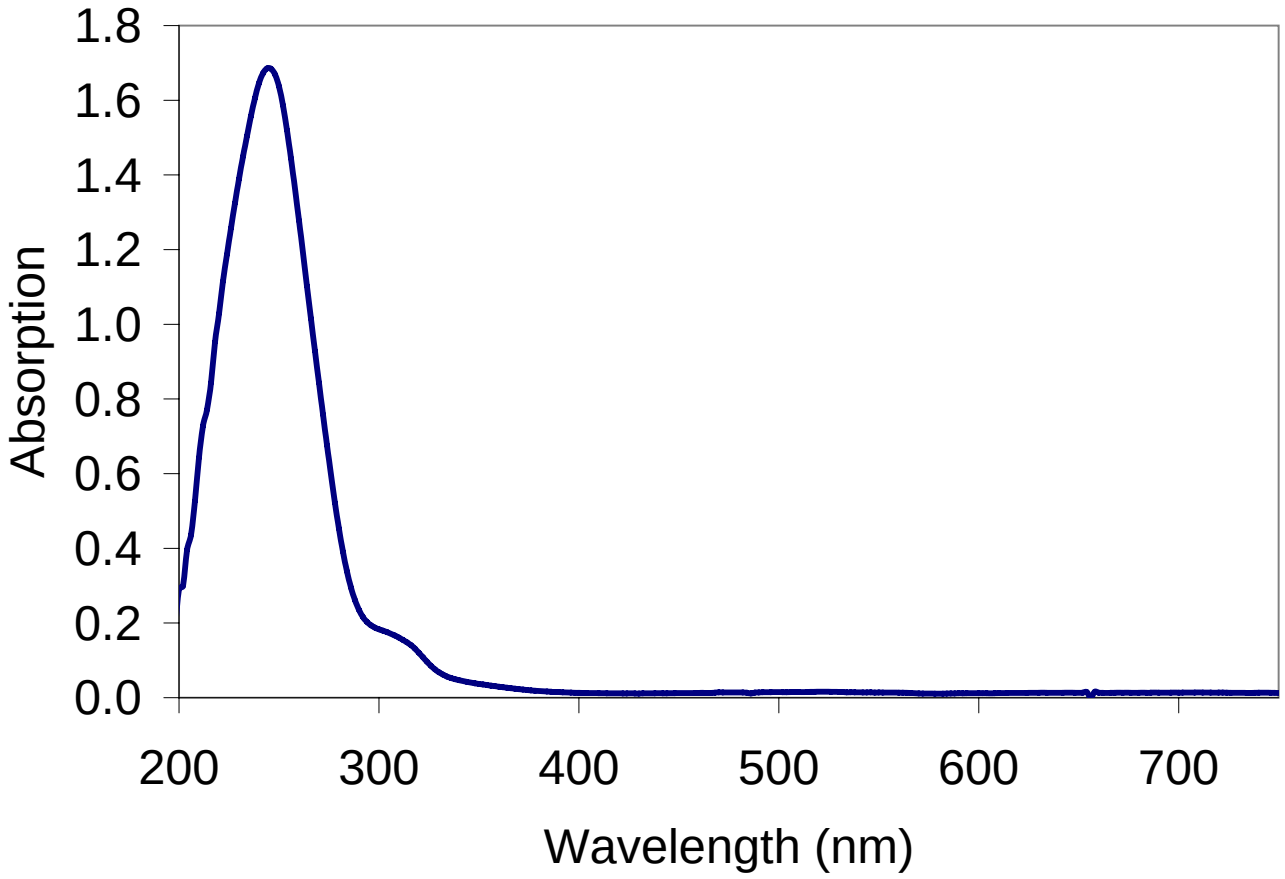


**FIGURE 3.6** Absorption of DNB-OH (0.1 mM) in 0.1 M $Na_2CO_3$ aqueous solution at pH 9.6.

The DNB-OH molecule has a strong absorption peak at 246 nm in 0.1 M $Na_2CO_3$ aqueous solution at pH 9.6 with no overlapping absorption in the 454 nm region where $RuNH_2$ absorbs (Figures 3.2 and 3.6). This allows for the content of dye and quencher on the polymer to be determined independently of each other. The extinction coefficient of DNB-OH was found to equal 15,300 $\pm 20\ M^{-1}cm^{-1}$ nm at 246 nm in a 0.1 M $Na_2CO_3$ aqueous solution at pH 9.6.

A Stern-Volmer plot describing the quenching of $RuNH_2$ by DNB-OH, Figure 3.7, shows the

ratio of the luminescence intensity without quencher ($I_o$) to that with quencher (I) as a function of quencher concentration. A straight line is obtained. The quenching rate constant can be obtained from the slope of this plot according to Equation 3.3 where $k_q$ is the quenching rate constant and $\tau$ is the lifetime of $RuNH_2$.[26]

$$k_q = \frac{slope}{\tau} \tag{3.3}$$

The Stern-Volmer plot shown in Figure 3.7 has a slope of 1550 $\pm$50 $M^{-1}$. Since $RuNH_2$ has a lifetime of 570 ns, the resulting quenching rate constant equals $2.7 \times 10^9 \pm 2 \times 10^8$ $M^{-1}s^{-1}$. The rate constant at which pyrene quenches itself in cyclohexane is $6.7 \times 10^9$ $M^{-1}s^{-1}$.[8] Although the quenching rate constant of pyrene is about twice as large as that of DNB-OH, a rate constant of $2.7 \times 10^9 \pm 130\ M^{-1}s^{-1}$ represents a strong quenching rate constant that is only three times smaller than the maximum value of $10^{10}$ $M^{-1}s^{-1}$ expected for a diffusion-controlled reaction taking place in water.[32] For a solution of $RuNH_2$ (10 $\mu$M) in DMF, the addition of 0.2 $\mu$M of DNB-OH caused the luminescence intensity to decrease by 40%, a decrease similar to that observed for the lifetime of $RuNH_2$ which decreased from 965 ns to 600 ns (Figure 3.4). Since both the luminescence intensity and the lifetime decreased by the same amount (within experimental error), the quenching mechanism must be collisional.[26] Therefore, DNB-OH was chosen as the quencher of the $RuNH_2$ dye for this study.

The second requirement for the quencher is that it be water soluble. The solubility of DNB-OH in water was $5 \times 10^{-3}$ mol/L. This is approximately four orders of magnitude larger than the

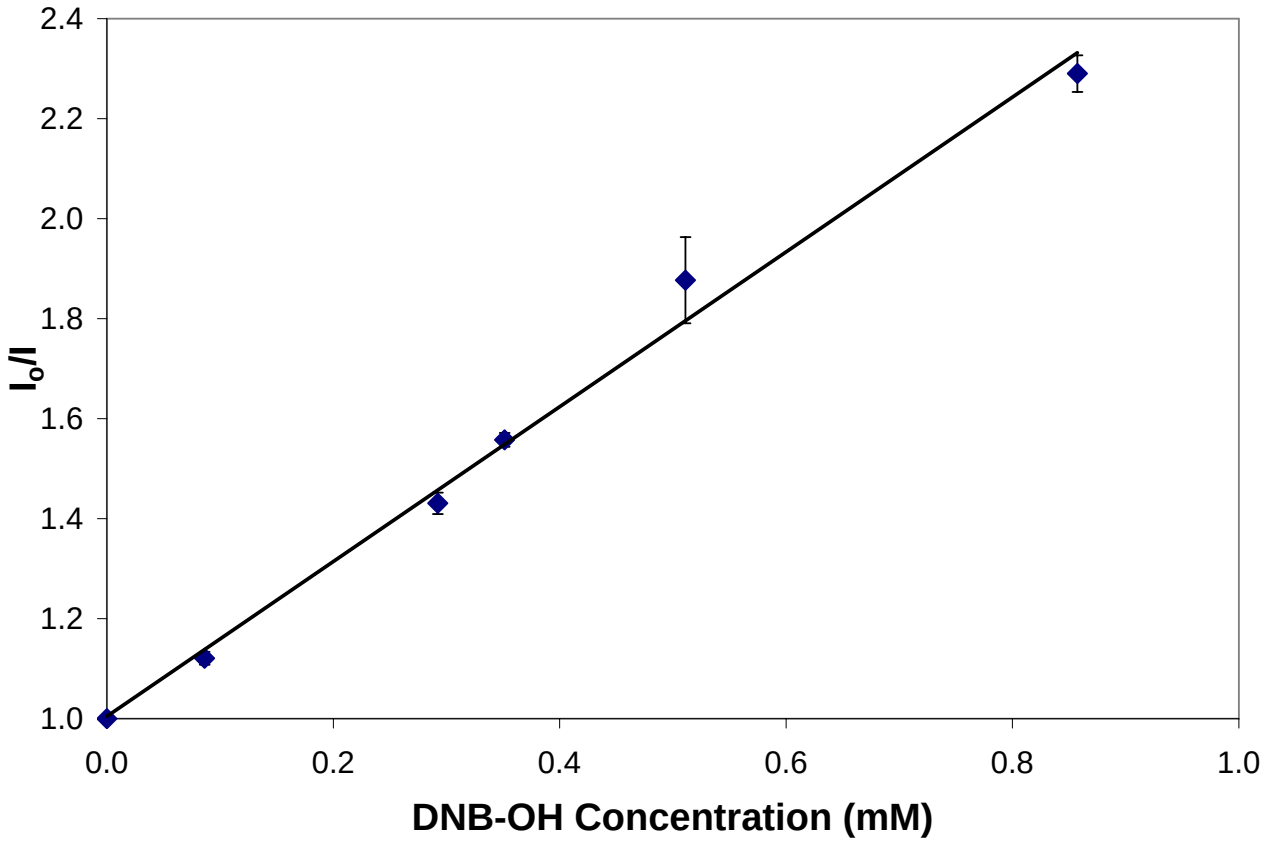


**FIGURE 3.7** Stern-Volmer plot for the quenching of $RuNH_2$ luminescence by DNB-OH in deaerated 0.1 M $Na_2CO_3$ aqueous solution at pH 9.6. $\lambda_{ex} = 454$ nm, $\lambda_{em} = 600 - 620$ nm, [$RuNH_2$] = 47 $\mu$M.

solubility of pyrene in water. Hence, this quencher satisfies the solubility requirement.

Finally, the quencher needs to be covalently attached to the polymer. Coupling of a small molecule to a polymer can be accomplished using an active ester group. The alcohol would then be connected to the backbone via an ester linkage. The ultimate goal of this research is to be able to study polymers labelled with the dye and quencher in water at varying pH values and temperatures. Unfortunately, ester linkages are hydrolyzable under acidic and basic conditions, which introduces

the possibility that the amount of quencher attached to the polymer could decrease over time under these conditions. This would make it impossible to obtain reliable information on quenching of the dye by DNB-OH, since cleavage of the quencher over time would reduce the quencher content. Conversion of the alcohol group to an amine results in the quencher being attached to the polymer via a much more stable amide linker.

The first synthetic route proposed is illustrated in Scheme 3.3. The alcohol is oxidized to an aldehyde[33] and reductive amination[34] of the aldehyde yields 3,5-dinitrobenzylamine (DNB-$NH_2$). Although the aldehyde was synthesized successfully, conversion of the aldehyde to the amine (**a**) was unsuccessful. By GC-MS, it appeared that the amine was synthesized. However reduction of the aldehyde to the original alcohol also occured. The amine (**a**) was never successfully purified though and further attempts at synthesizing it were unsuccessful. Thus, a second synthesis method was proposed.

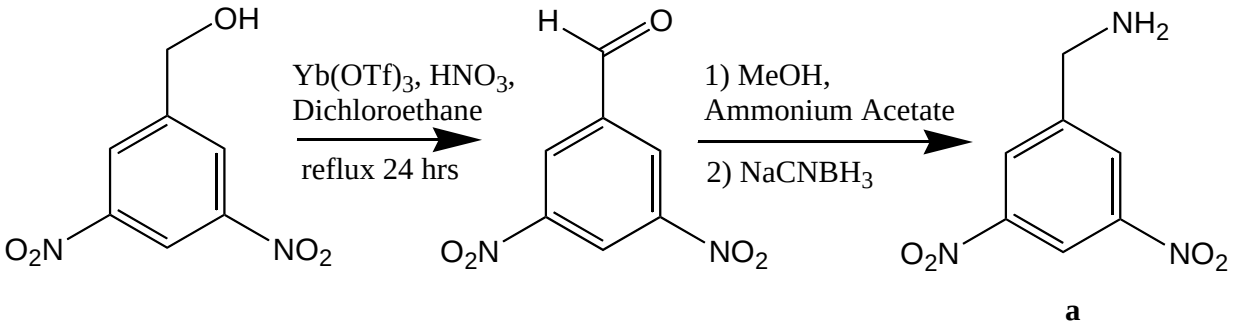


**SCHEME 3.3** Synthesis of 3,5-dinitrobenzylamine (DNB-$NH_2$) from 3,5-dinitrobenzyl alcohol (DNB-OH)

The second reaction scheme proposed is shown in Scheme 3.5 where the amine is derived

from a halide.[35] 3,5-Dinitrobenzyl bromide (DNB-Br) was synthesized according to Scheme 3.4[36] and 3,5-dinitrobenzyl chloride (DNB-Cl) was purchased from Sigma-Aldrich. Both products were used to synthesize 3,5-dinitrobenzyl-tritylamine using two equivalents of tritylamine. The first equivalent acts as a nucleophile while the second equvalent acts as a base. 3,5-Dinitrobenzyl-tritylamine was deprotected with trifluoroacetic acid (TFA) to yield DNB-$NH_2$. The trityl cation side product was reacted with methanol to produce tritylmethyl ether. Addition of HCl in methanol yielded the amine salt which could be more easily purified.

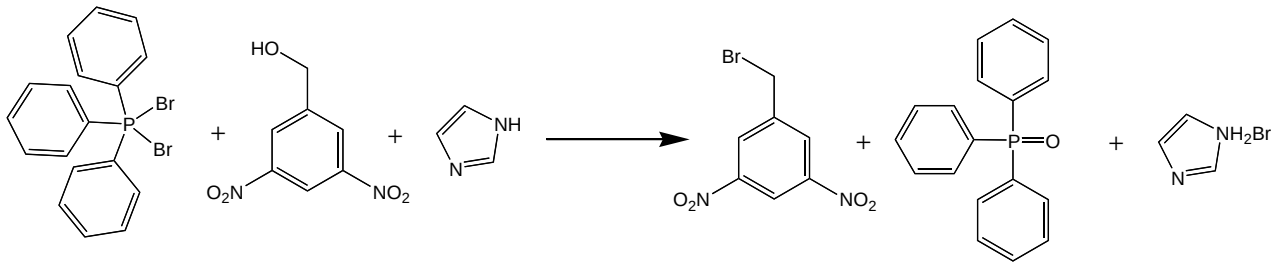


**SCHEME 3.4** Synthesis of 3,5-dinitrobenzyl bromide (DNB-Br) from 3,5-dinitrobenzyl alcohol (DNB-OH)

Originally, DNB-Br was used to synthesize the benzyl-tritylamine. Unfortunately, the reaction starting from DNB-Br was incomplete and the purification of 3,5-dinitrobenzyl-tritylamine was never accomplished. Conversion of 3,5-dinitrobenzyl-tritylamine to DNB-$NH_2$ (**b**) was still attempted however, and characterization by ESI-MS shown in Figure A.5 demonstrated that the desired product was obtained. After several attempts at synthesizing the benzyl-tritylamine from DNB-Br, it was realized that although DNB-Br was not commercially available, DNB-Cl was, and, since chlorine is also a good leaving group, subsequent attempts used DNB-Cl as the starting

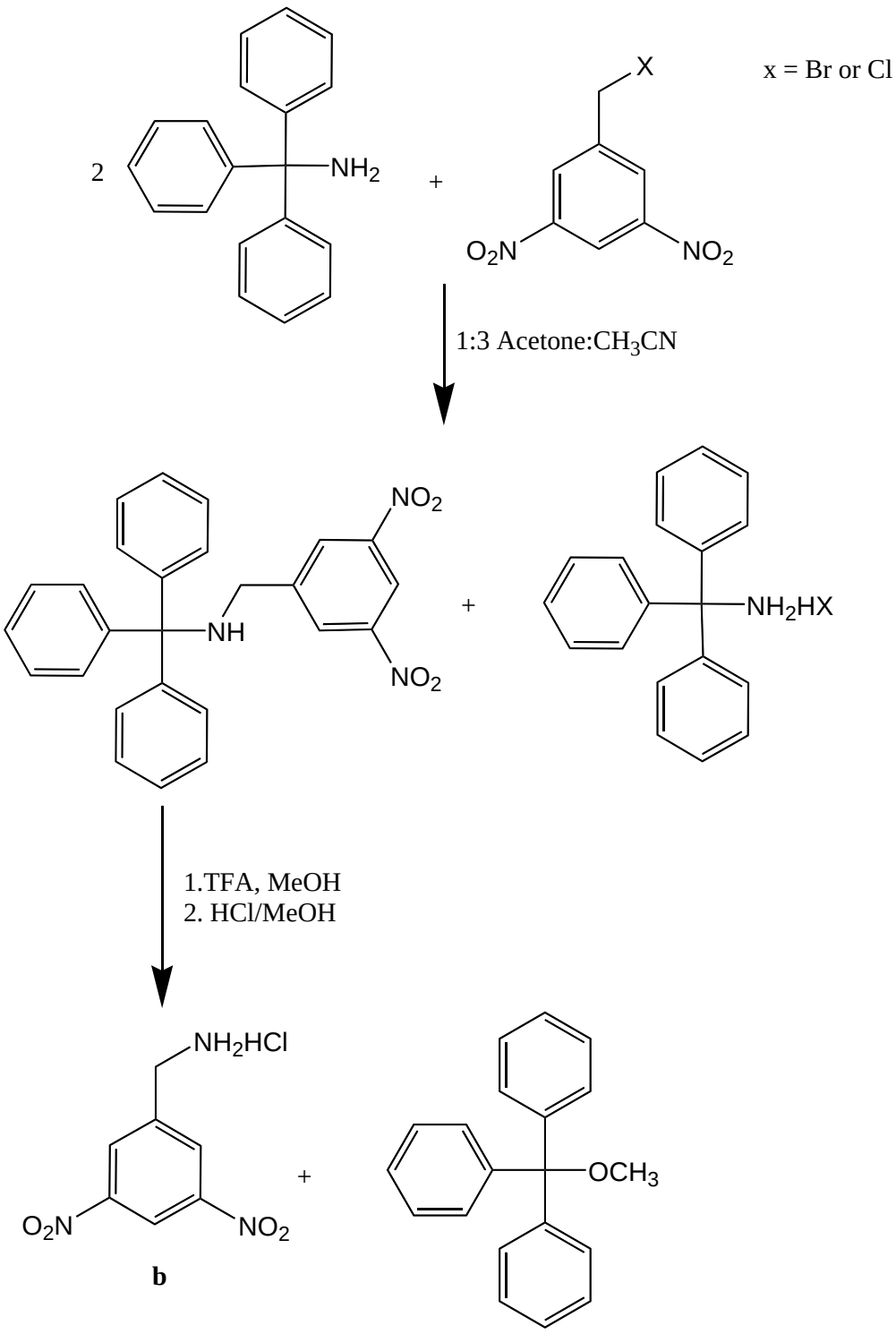


**SCHEME 3.5** Synthesis of 3,5-dinitrobenzylamine (DNB-$NH_2$) from 3,5-dinitrobenzyl halide (DNB-X)

material. In this approach, one less reaction step was required to obtain DNB-$NH_2$. Synthesis of 3,5-dinitrobenzyl-tritylamine from DNB-Cl was much cleaner and the reaction was always complete. The desired 3,5-dinitrobenzyl-tritylamine product was successfully purified and DNB-$NH_2$ was synthesized. The MS, $^{1}$H NMR, and $^{13}$C NMR spectra of DNB-$NH_2$ are shown in Figures A.6 - A.8 of Appendix A, respectively.

Some properties of $RuNH_2$, DNB-OH and pyrene are summarized and compared in Table 3.1. Although polymers are not labelled with these molecules directly but rather with derivatives of the molecules, comparison of the original compounds provides a basic understanding of the similarities and differences between the systems. The volumes of the molecules were approximated based on published crystallography data. The volume of a crystal unit cell was divided by the number of molecules per unit cell in order to obtain the volume occupied by a single molecule. Table 3.1 indicates that the volume occupied by the quencher and the pyrene molecules is approximately the same. This is important because a larger label is expected to affect the dynamics of a polymer chain to a larger extent than a small label. Since comparison of a pyrene labelled polymer with a DNB-OH labelled polymer is desired, the similar volumes of pyrene and DNB-OH should induce negligible differences in the polymer dynamics. The volume of $RuNH_2$, however, is approximately 3.5 times larger than that of pyrene. Although this is a large difference, the amount of dye to be attached to the polymer chain is so low that it is not expected to have a significant impact on the polymer dynamics. As mentioned previously, $RuNH_2$ and DNB-OH are significantly more soluble in water than pyrene and the quenching rate constant for DNB-OH is sufficiently large despite being less than that of pyrene. The extinction coefficients for $RuNH_2$ and DNB-OH are also less

than that of pyrene but they are still large enough that luminescence studies can be performed. Of significant importance between the systems is the difference in lifetimes between $RuNH_2$ and pyrene. The lifetime of pyrene in cyclohexane, which is the solvent in which pyrene takes its longest lifetime, is 450 ns. This is the longest lifetime that can be obtained for pyrene.[8] On the other hand, $RuNH_2$ has a lifetime of 570 ns in 0.1 M $Na_2CO_3$ aqueous solution at pH 9.6 and up to 965 ns in DMF. This means that not only can water-soluble polymers be studied with $RuNH_2$ but also much slower polymer dynamics can be observed.

**TABLE 3.1** Comparison of $RuNH_2$, DNB-OH, and pyrene.

| | $RuNH_2$[a] | DNB-OH[a] | Pyrene[b] |
|---|---|---|---|
| Volume (Å) | 890 [37] | 210 [38] | 260 [39] |
| Water Solubility (mol/L) | $1 \times 10^{-3}$ | $5 \times 10^{-3}$ | $6.8 \times 10^{-7}$ [30] |
| $\lambda_{ex}$ (nm) | 454 | 240 | 336 [40] |
| Extinction Coefficient | 13,800 | 15,300 | 54,000 [40] |
| $k_q(M^{-1}s^{-1})$ | – | $2.7 \times 10^9 \pm 130$ | $6.7 \times 10^9$ [8] |
| $\lambda_{em}$ (nm) | 610 | – | 372 [40] |
| Deaerated luminescence lifetime (ns) | 570 | – | 450 [8] |

[a] These measurements were obtained using a 0.1 M $Na_2CO_3$ aqueous solution at pH 9.6.

[b] These values are for pyrene solutions in cyclohexane and were obtained from the indicated literature references.

# 4

# Polymer Synthesis and Characterization

## 4.1 Introduction

Earlier work with poly(*N*,*N*-dimethylacrylamide) (PDMA) labelled with pyrene involved studying its dynamics by applying the Fluorescence Blob Model.[11,12] The polymers synthesized had weight-average molecular weights in the 80-300 kg/mol range and pyrene contents ranging from 0.2 to 7.3 mol%.[11,12] For the present study, PDMA was synthesized as a copolymer of *N*,*N*-dimethylacrylamide (DMA) and *N*-acryloxysuccinimide (NASI). The NASI sites are required in order to couple the dye, RuNCS, and quencher, DNB-$NH_2$, to the polymer backbone. The fully labelled end product polymer shown in Figure 4.1 has the dye attached to the polymer backbone via a diamine linker. This diamine linker is necessary to attach RuNCS as well as to minimize steric hindrance between the bulky dye and the polymer.

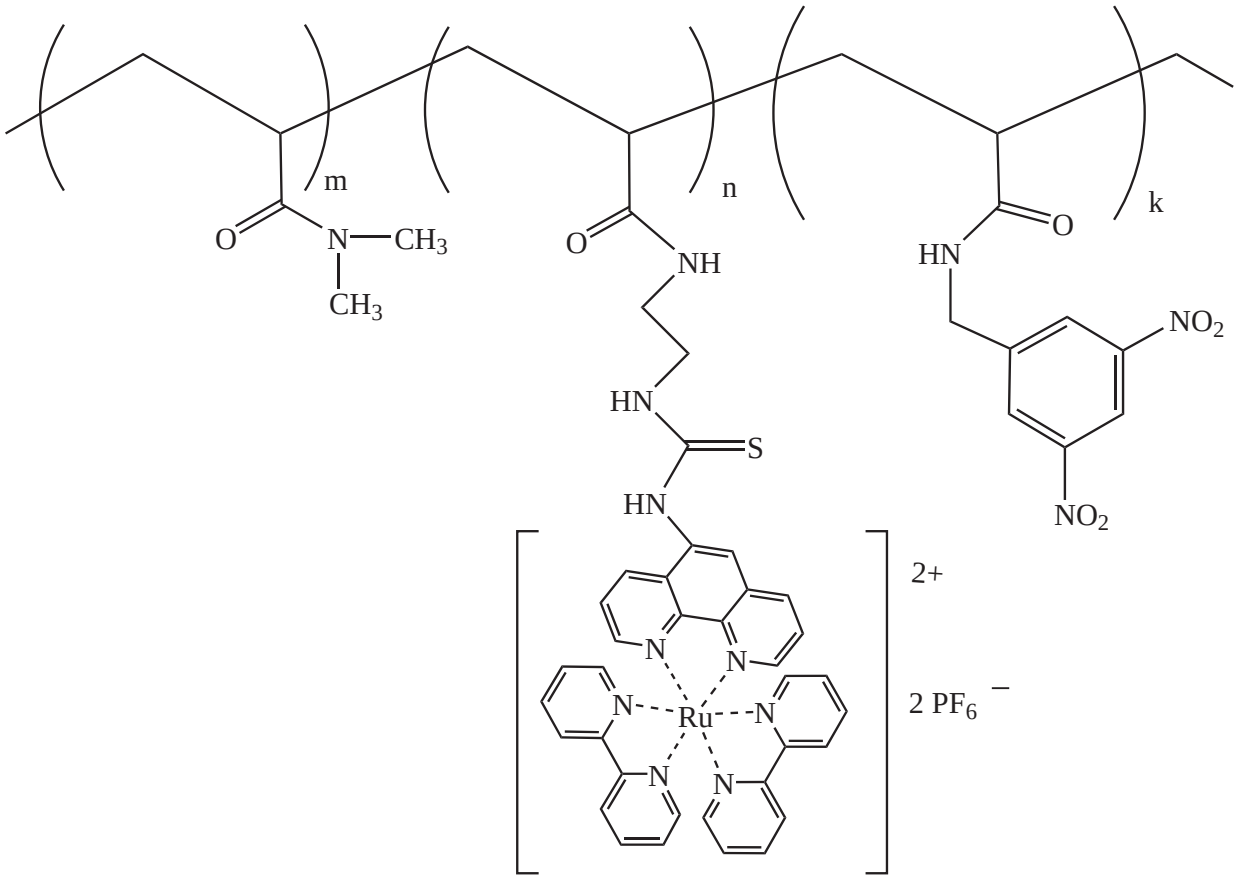


**FIGURE 4.1** Polymer labelled with RuNCS and DNB-$NH_2$

## 4.2 Results and Discussion

### 4.2.1 Copolymerization of DMA and NASI

A copolymer of DMA and NASI was prepared such that the active ester groups of the NASI monomer could be utilized for attaching the dye and quencher. The polymer was prepared by radical polymerization using $\alpha, \alpha'$-azobisisobutyronitrile (AIBN) as the initiator (Scheme 4.1). The study of any labelled polymer requires that the polymer composition be homogenous throughout

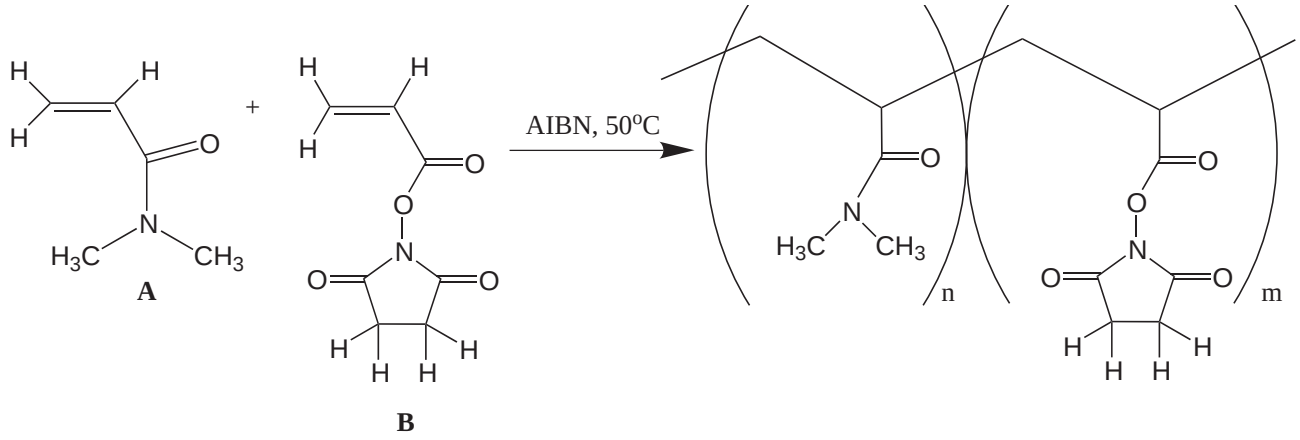


**SCHEME 4.1** Synthesis of a copolymer of DMA (A) and NASI (B) by radical copolymerization. *m* and *n* represent the mole fractions of NASI and DMA monomers, respectively.

the synthesis. In order to verify that no drift in monomer incorporation existed, the copolymerization was monitored over time by $^1$H NMR.

By $^1$H NMR, the alkene protons of the two monomers can be differentiated and individually integrated, when deuterated acetone is used as the NMR solvent, as evident in Figures B.1 and B.2 in Appendix B. Therefore, a $^1$H NMR experiment was designed to determine the concentration of the monomers in the feed at several times throughout the reaction. This required an internal integration standard which would not react with the monomers and whose signal could be used as a reference to determine their concentration. For this purpose, a glass insert containing trifluoroacetic acid (TFA) was used. TFA produced a strong singlet at 11.2 ppm - well out of the range of the other peaks. Since TFA was contained in the glass insert, it did not react with the monomers. Also, the same insert was used in each NMR tube so that the amount of TFA in the NMR samples

remained constant. The NMR solutions were prepared by removing a small amount ($\sim$15-100 mg) of the reaction solution from the reaction flask, via a syringe, and injecting it into an NMR tube of known mass. The exact amount of reaction mixture was measured by mass, as well as the amount of deuterated solvent added to the mixture. It is important to note that by preparing the NMR solution in this way, the solution also contained everything in the reaction mixture including the reaction solvent (DMF) and initiator (AIBN). Since a substantial amount of reaction solvent was present in the NMR solution, the proton peaks are shifted slightly compared to those obtained in an NMR spectrum of only the monomers in deuterated acetone. Several solutions for NMR measurements were prepared in this way over the course of the reaction. The solvents, DMF and acetone, were selected based on several criteria. The reaction solvent, DMF, must not evaporate, must solubilize both the monomers and polymer, and the solvent peaks in the $^1$H NMR spectrum must not overlap the alkene peaks of the monomers. The deuterated solvent, in this case acetone, must be miscible with the reaction solvent, DMF, and must enable the spectral resolution of the monomers from one another.

The $^1$H NMR spectra of the solutions with the TFA insert were acquired, integrated, and analyzed to determine conversion. Since the initial concentration of the DMA, $[DMA]_0$, and NASI , $[NASI]_0$, monomers is known, the monomer concentrations at any given time can be calculated from Equations 4.3 and 4.4 using the integration constants $\nu$ and $\mu$ given in Equations 4.1 and 4.2. In Equations 4.1 - 4.4, $I_o$ and $I_t$ represent the NMR peak intensities at time = 0 and time = *t*, respectively. The volumes of the reaction solution at time *t* and the NMR mixture are referred to as $V_{rxn_t}$ and $V_{NMR}$, respectively. $V_{rxn_0}$ represents the volume of the reaction at

time = 0. The volumes $V_{rxn_0}$ and $V_{rxn_t}$ were determined by dividing the mass of reaction mixture taken from the reaction vessel by the density of the reaction solvent, DMF in this case.

$$\nu = \frac{[DMA]_0 \times V_{rxn_0}}{I_0(DMA)V_{NMR}} \tag{4.1}$$

$$\mu = \frac{[NASI]_0 \times V_{rxn_0}}{I_0(NASI)V_{NMR}} \tag{4.2}$$

$$[DMA]_t = \nu \times I_t(DMA) \times \frac{V_{NMR}}{V_{rxn_t}} \tag{4.3}$$

$$[NASI]_t = \mu \times I_t(NASI) \times \frac{V_{NMR}}{V_{rxn_t}} \tag{4.4}$$

From the concentration of DMA at a given time,$[DMA]_t$, the concentration of NASI at a given time, $[NASI]_t$, $[DMA]_0$, and $[NASI]_0$, the average conversion for both monomers at any given time can be calculated according to Equation 4.5.

$$Conversion = \frac{([DMA]_0 - [DMA]_t) + ([NASI]_0 - [NASI]_t)}{[DMA]_0 + [NASI]_0} \tag{4.5}$$

A plot of the molar fractions of monomer in the feed versus conversion is shown in Figure 4.2. This plot demonstrates that the amount of NASI in the feed decreases as conversion increases. In

other words, the NASI monomer was preferentially incorporated into the copolymer. This experimentally obtained trend agrees with the theoretical trend obtained by using the monomer reactivity ratios of 0.36 and 0.60 for DMA and NASI, respectively.[41] The theoretical trends shown in Figure 4.2 were determined according to equation 4.6[42]

$$p = 1 - \frac{M}{M_0} = 1 - \left[\frac{f_1}{(f_1)_0}\right]^{\alpha} \left[\frac{f_2}{(f_2)_0}\right]^{\beta} \left[\frac{(f_1)_0 - \delta}{(f_1) - \delta}\right]^{\gamma} \tag{4.6}$$

where M is the total number of moles of the two monomers at time *t*, $f_1$ and $f_2$ are the instantaneous feed compositions of monomers 1 and 2, respectively, and the zero subcripts indicate the initial quantities at *t* = 0. The constants $\alpha, \beta, \gamma$, and $\delta$ are given by

$$\alpha = \frac{r_2}{(1 - r_2)} \tag{4.7}$$

$$\beta = \frac{r_1}{(1 - r_1)} \tag{4.8}$$

$$\gamma = \frac{r_1 r_2}{(1 - r_1)(1 - r_2)} \tag{4.9}$$

$$\delta = \frac{1 - r_2}{(2 - r_1 - r_2)} \tag{4.10}$$

where $r_1$ and $r_2$ are the reactivity ratios of monomers 1 and 2, respectively.

The reactivity ratios used in Figure 4.2 were originally determined by $^1$H NMR spectroscopy for reversible addition-fragmentation chain transfer (RAFT) polymerization of these two monomers.[41] Because NASI is preferrentially incorporated, the polymerization reactions for this study were only

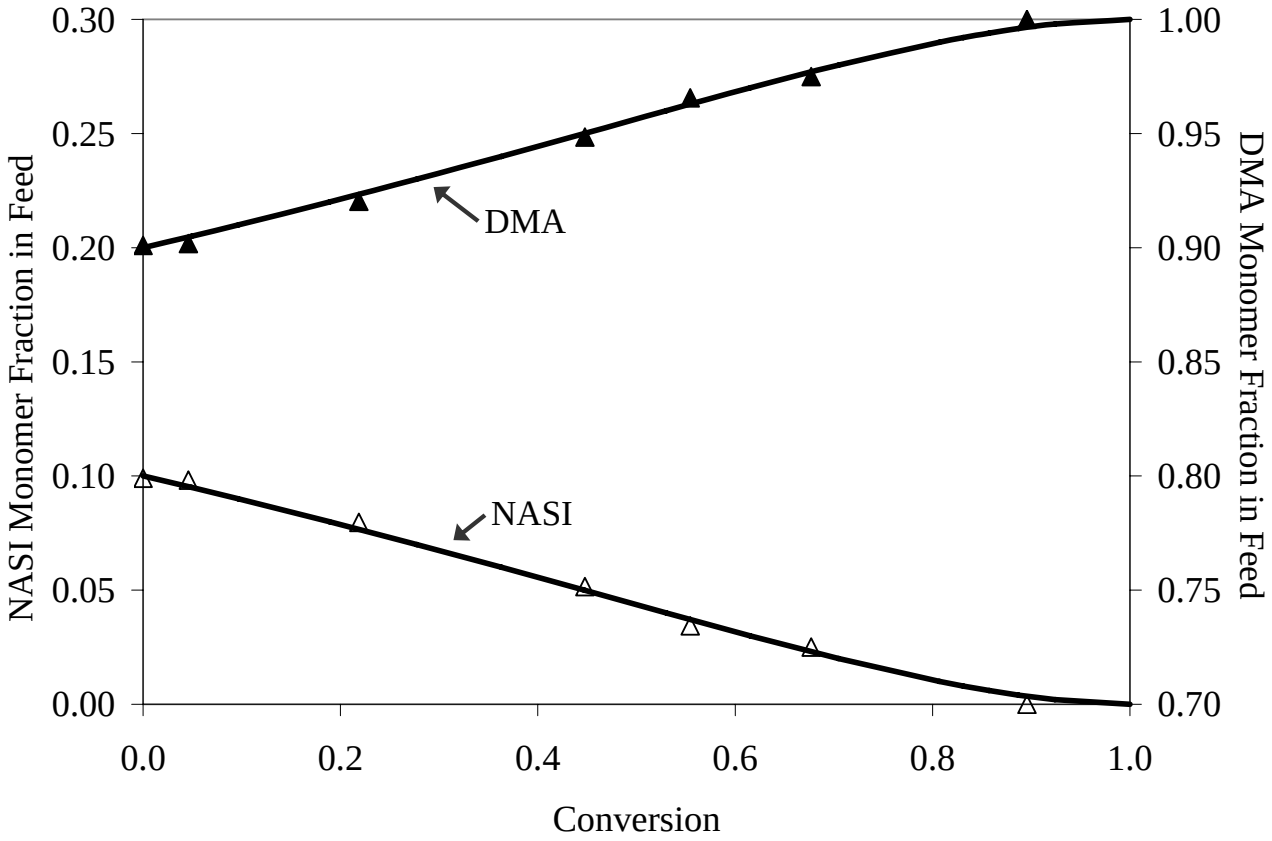


**FIGURE 4.2** Experimentally (△) and theoretically (—) obtained molar fraction of DMA (filled) and NASI (hollow) in the feed as a function of conversion.

carried out up to a conversion of 0.2. Within the 0 - 0.2 conversion range, the amount of monomer in the feed only drifts by 20% and therefore, all chains are expected to contain a similar average number of NASI monomers.

### 4.2.2 Labelling the Polymer with the Dye and Quencher

Once a copolymer was synthesized, several labelling steps needed to be performed. A schematic representation of the full labelling process is given in Schemes 4.2 and 4.3. The first step con-

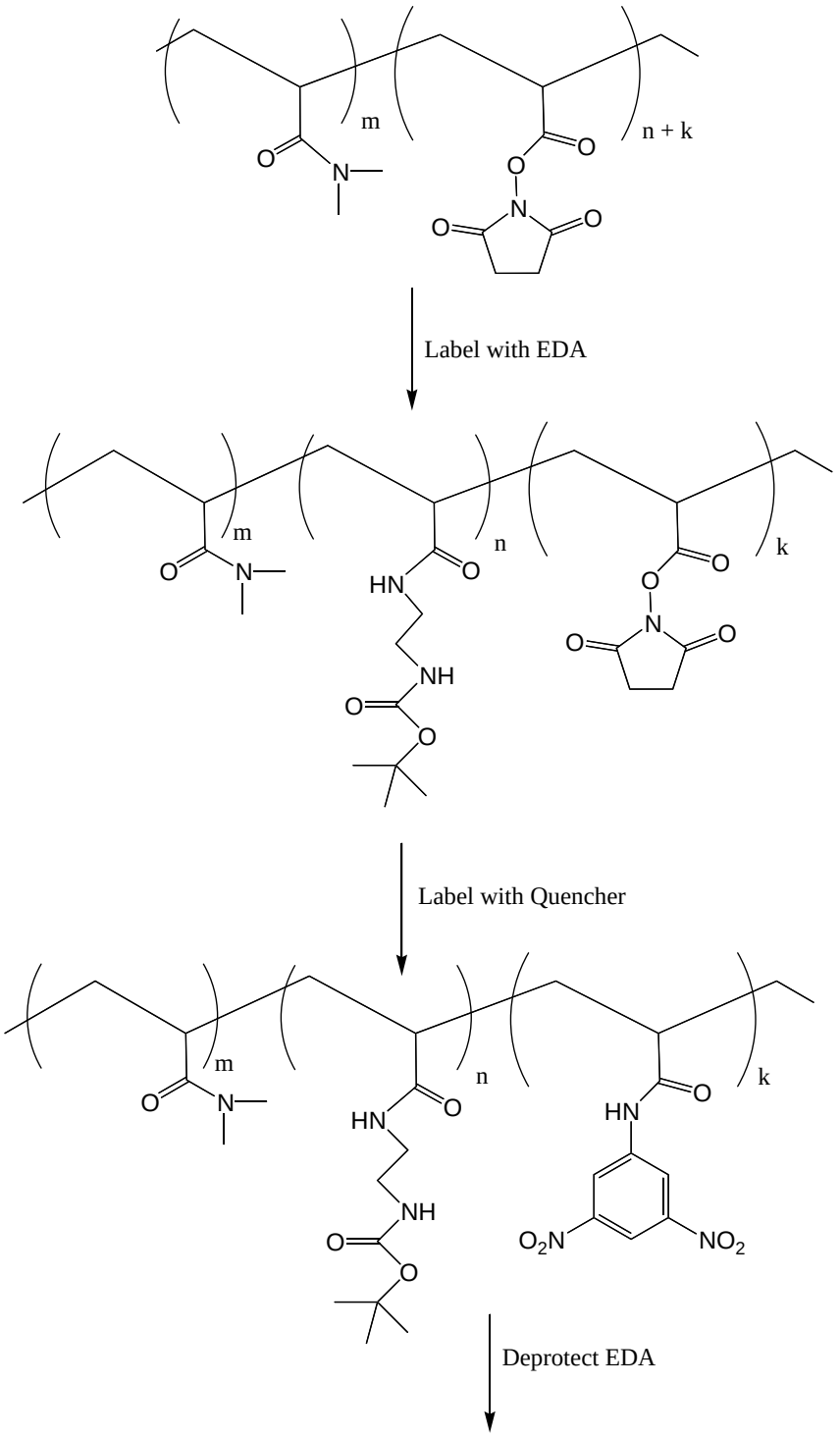


**SCHEME 4.2** Labelling procedure for DMA/NASI copolymer.

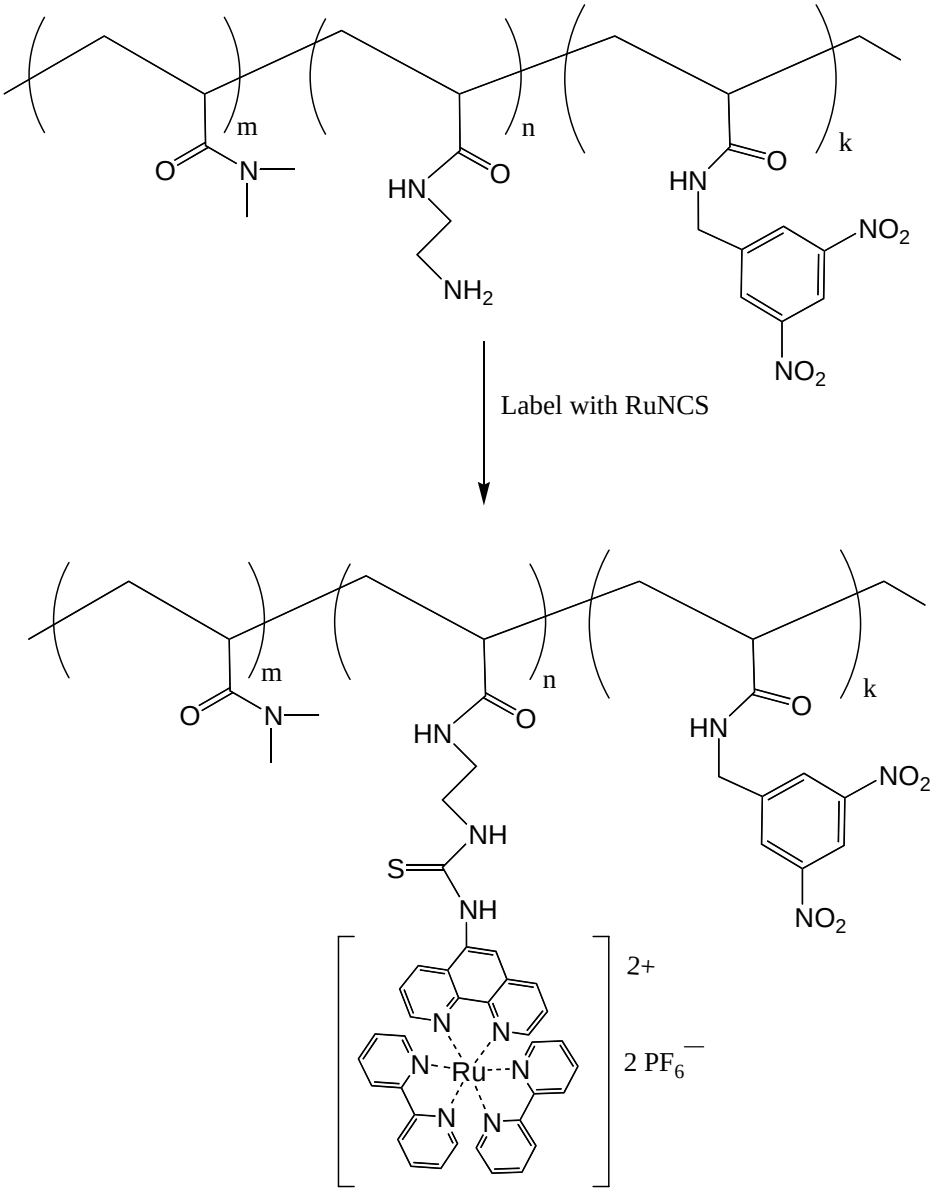


**SCHEME 4.3** Labelling procedure for DMA/NASI copolymer continued.

sisted in attaching *N*-BOC-1,2-ethylenediamine (EDA) – the linker connecting the RuNCS dye to the polymer. One of the primary amines of EDA was protected with a *t*-butoxycarbonyl (BOC) group to prevent crosslinking between NASI monomers. After the EDA linker was coupled to the polymer backbone at some of the NASI sites, the remaining NASI sites were reacted with the 3,5-dinitrobenzylamine quencher. At this point, all the NASI groups were assumed to have reacted and EDA was deprotected. The deprotected primary amine was then allowed to react with the RuNCS dye.

In order to couple the EDA and quencher to the polymer backbone, a base must be used. Since the coupling reactions were done in DMF, triethylamine was chosen as the base. Preliminary reactions with $RuNH_2$ and triethylamine showed that the dye degraded in the presence of triethylamine possibly by displacing the ligands from the Ru center. It was assumed that a similar reaction would occur with RuNCS. Therefore, extensive dialysis of the polymer sample was required after labelling it with the EDA linker and quencher to ensure that no triethylamine remained.

The final amount of labelling was determined by UV absorption. In the case of RuNCS, the extinction coefficient of $RuNH_2$ was used since RuNCS was always obtained as a mixture with $RuNH_2$ and the dimer. Absorption spectra of the polymer indicate a quantitative labelling yield of RuNCS and a 6% yield for labelling with DNB-$NH_2$. Therefore, this method of labelling PDMA is feasible however the efficiency for quencher attachment is low. It is important to note however, that crosslinking of the polymer does occur with minimal exposure to moisture if not all NASI sites have reacted.[14] Therefore, it is important that the polymer be immediately reacted with EDA

and/or quencher in a dry solvent to minimize crosslinking of the copolymer.

### 4.2.3 Polymer Luminescence

Although the final goal of this research was to analyze the luminescence of water-soluble polymer PDMA in water, the behaviour of the labelled polymer must first be investigated in DMF. Since pyrene-labelled PDMA in DMF has already been studied according to the FBM, comparisons between the two labelled polymer systems must be made. For this reason, the luminescence of the RuNCS and DNB-$NH_2$ labelled polymers were first acquired in DMF. Several copolymers were synthesized and labelled with the dye and quencher. A polymer labelled only with RuNCS was also synthesized. The luminescence decay of PDMA labelled with 0.03 mol% RuNCS (where mol% represents the ratio of the number of moles of monomer labelled with the dye over the total number of moles of monomer making up the polymer) in DMF was acquired using a NanoLED excitation at 460 nm and a repetition rate of 100 kHz (Figure 4.3). A time per channel of 10.08 ns was used. The luminescence was collected at $\lambda_{em}$ = 610 nm. Fitting the decay with a sum of three exponentials yielded a $\chi^2$ = 1.07. A short decay time of 20 ns was obtained with little accuracy since it was too close to the time per channel of the decay. The two other decay times of 170 ns and 1000 ns were better resolved and had pre-exponential weights of 0.11 and 0.72, respectively. The short decay time could be due to light scattering from the polymer solution, or to rapid quenching of the dye by the polymer backbone. Most importantly, the strongest contribution to the decay was the lifetime of 1000 ns, characteristic of the free dye in DMF. Also, the data shown in Figure 4.3 demonstrates that PDMA was successfully labelled with a water-soluble long-lived dye and hence

the primary goal of this project was accomplished.

A NASI/DMA copolymer was synthesized and labelled with RuNCS and DNB-$NH_2$. The dye content of the polymer was 0.01 mol% or $\lambda_d$ = 1.5 $\mu$mol/g (see appendix C to convert mol% of dye to $\mu$mol/g dye content ($\lambda_d$)). The quencher content was 1.1 mol% or $\lambda_q$ = 32 $\mu$mol/g. The labelling yield for RuNCS was quantitative while that of DNB-$NH_2$ was 6%. Unfortunately, during the dialysis of the polymer, the sample was contaminated with 1-pyrenemethylamine. Extensive dialysis was not successful in removing pyrene from the samples as evidenced by both absorption and fluorescence measurements. The presence of 1-pyrenemethylamine in the sample can have several consequences. First of all, 1-pyrenemethylamine can react at free NASI sites. However, this coupling reaction requires basic conditions so that the extent of this reaction is likely to be minimal. Second, it is possible that benzylamines, such as the one found on 1-pyrenemethylamine, can displace the bipyridine and/or phenanthroline ligands from the dye as would triethylamine. This would change the absorption and emission properties of the dye and affect the quenching results. Finally, it is possible that 1-pyrenemethylamine quenches RuNCS which would also affect the quenching results of the polymer.

Nevertheless, a luminescence decay of the polymer was acquired, in DMF, using a time per channel of 2.04 ns and excitation and emission wavelengths of 460 nm and 610 nm, respectively (Figure 4.3). The luminescence decay was fitted with a sum of three exponentials yielding a $\chi^2$ of 1.06. The three decay times equalled 3 ns, 10 ns, and 915 ns with pre-exponential weights of 0.86, 0.10 and 0.04, respectively. The long decay time is similar to that of the unquenched RuNCS moi-

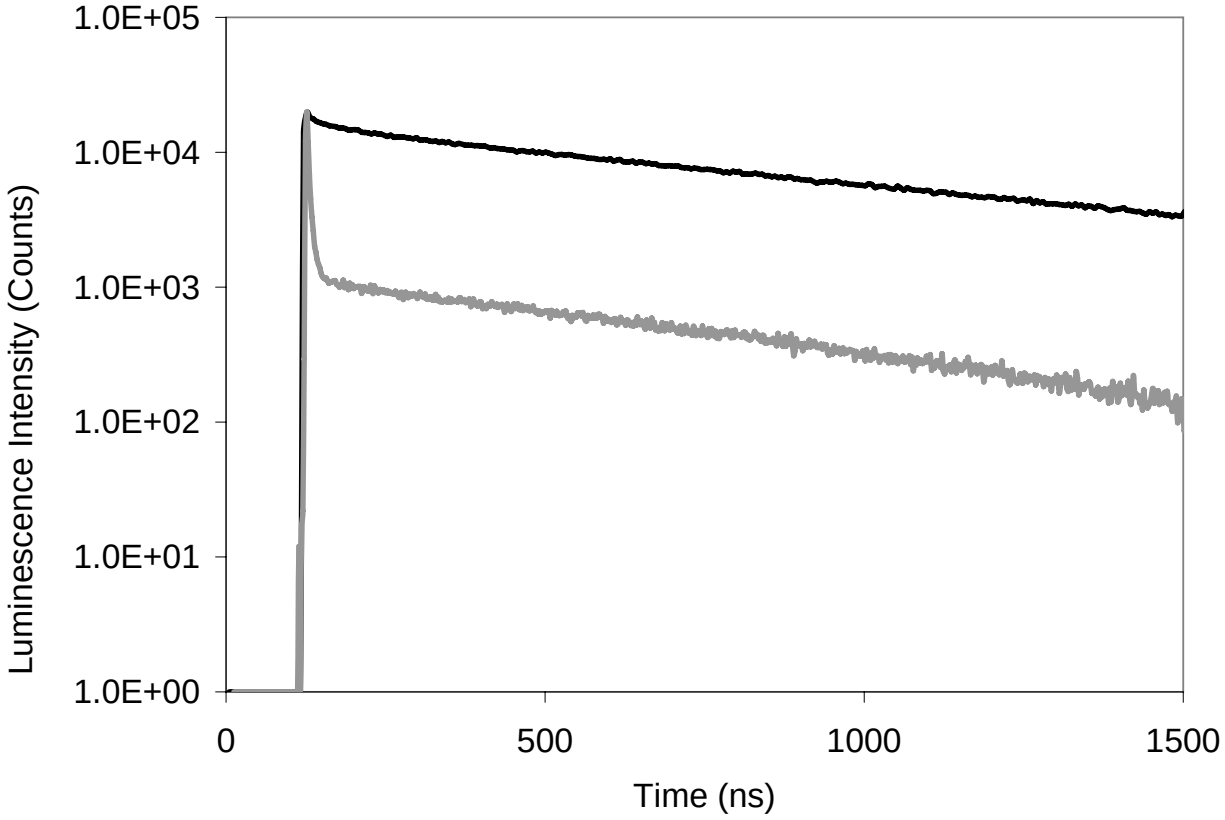


**FIGURE 4.3** Lifetime decay of PDMA labelled with 0.03 mol% RuNCS, in DMF, using NanoLED excitation with a repetition rate of 100 kHz and a time per channel of 5.07 ns (black line). ($\tau_1$ = 23 ns, $\tau_2$ = 170 ns, $\tau_3$ = 1000 ns, $a_1$ = 0.17, $a_2$ = 0.11, $a_3$ = 0.72, $\chi^2$ = 1.07). Lifetime decay of PDMA labelled with 0.01 mol% RuNCS and 1.1 mol% DNB-$NH_2$, in DMF, using NanoLED excitation with a repetition rate of 500 kHz and a time per channel of 2.04 ns. ($\tau_1$ = 3 ns, $\tau_2$ = 10 ns, $\tau_3$ = 915 ns, $a_1$ = 0.86, $a_2$ = 0.10, $a_3$ = 0.04, $\chi^2$ = 1.06). $\lambda_{ex}$ = 460 nm and $\lambda_{em}$ = 610 nm.

eties. The short decay times indicate that some quenching occurs on a very fast time scale – much too fast to be attributed to dynamic quenching. In fact, it seems that most of the RuNCS moieties are being quenched in a static manner although the exact weights of each lifetime will be inaccurate since the major contributor, the 3 ns lifetime, is too short to be resolved at a time per channel of 2.04 ns. This static quenching is most likely due to the formation of a complex between the excited dye and either DNB-$NH_2$ attached onto the backbone or the 1-pyrenemethylamine contaminant. It was hoped that the dinitrobenzyl quencher attached to the polymer via an amide linker would behave similarily to the dinitrobenzyl alcohol quencher. However, in light of the observed static quenching, it appears as though the amide quencher behaves more like 3,5-dinitroaniline. The quenching rate constant for 3,5-dinitroaniline and $RuNH_2$ was found to equal $3.7 \times 10^{11}$ $M^{-1}s^{-1}$ in 0.1 M $Na_2CO_3$ solution at pH 9.6. Since the maximum rate of diffusional encounter in water is $10^{10}$ $M^{-1}s^{-1}$, a rate constant on the order of $10^{11}$ $M^{-1}s^{-1}$ implies that static quenching is occuring. Therefore, it is possible that the amide linker changed the quenching properties of the quencher.

The luminescence spectra of the PDMA samples labelled with RuNCS only and with both RuNCS and DNB-$NH_2$ are compared in Figure 4.4. Introduction of the quencher onto the polymer results in a substantial decrease of luminescence intensity, however there was also a broadening of the emission spectra. This broadening was not observed for the quenching of $RuNH_2$ by DNB-OH shown in Figure 3.5 and indicates the formation of a new luminescent species - a result consistent with the luminescence decays shown in Figure 4.3. It remains to be seen whether this new species is due to the DNB-$NH_2$ quencher or 1-pyrenemethylamine. Conclusive results on the quenching

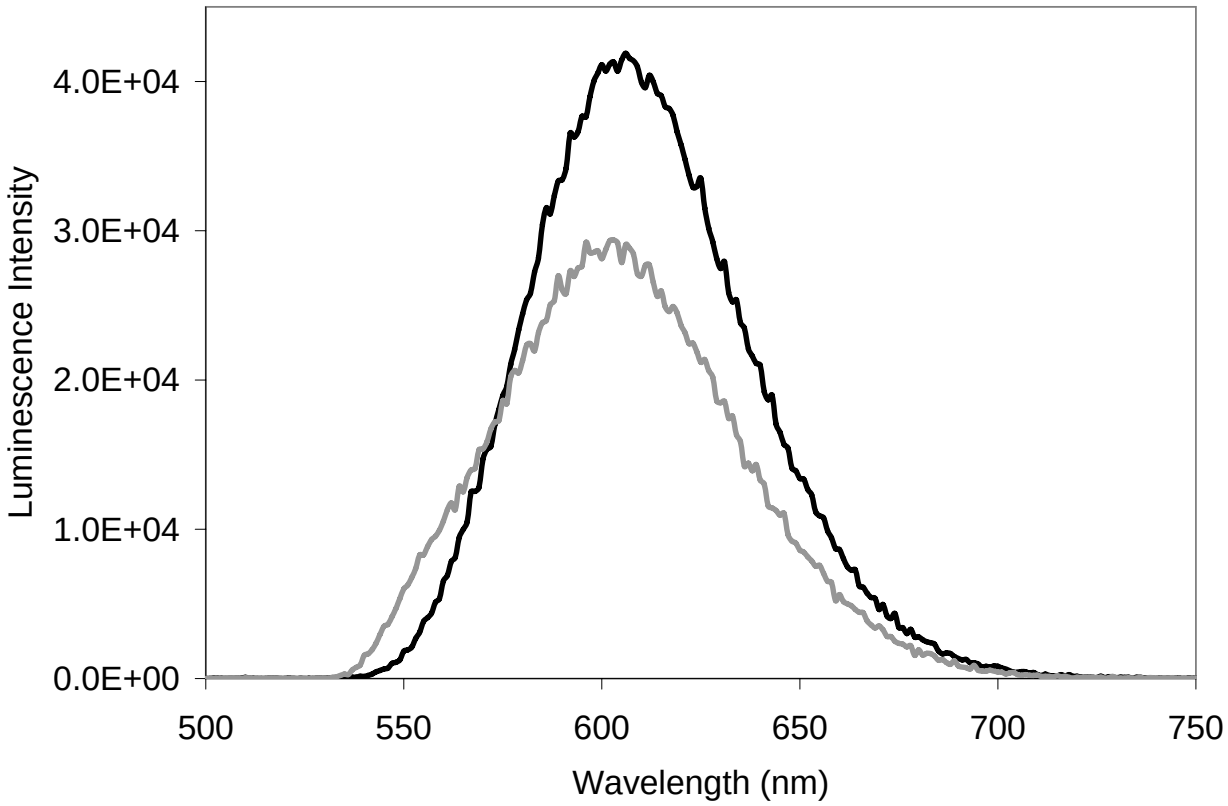


**FIGURE 4.4** Luminescence of PDMA labelled with 0.03 mol% RuNCS (black line). Luminescence of PDMA labelled with 0.01 mol% RuNCS and 1.1 mol% DNB-$NH_2$ in DMF (grey line). O.D. = 0.1, $\lambda_{ex}$ = 460 nm.

ability of 3,5-dinitrobenzylamine bound to the polymer via an amide linker could not be made from the data obtained so far due to the presence of an impurity. This will be possible upon obtaining a labelled polymer which is not contaminated with 1-pyrenemethylamine.

# 5

# Conclusions and Future Work

The objective of this research project was to determine the feasibility of labelling a water-soluble polymer with a water-soluble dye and quencher. The water-soluble dye chosen was $RuNH_2$. This dye was not only water-soluble but also soluble in several organic solvents (including ethyl acetate, acetone, acetonitrile, and DMF). $RuNH_2$ was characterized by UV and luminescence and found to have an absorption maximum at 454 nm in 0.1 M $Na_2CO_3$ aqueous solution at pH 9.6 and at 460 nm in DMF. In either solvent, the emission was broad, structureless, and centered around 610 nm. $RuNH_2$ was synthesized and converted to the isothiocyanate, RuNCS, which was then reactive enough to covalently bond to a polymer displaying primary amines. Several exploratory reactions with $RuNH_2$ revealed that it is stable if reacted with TFA but tertiary amines will complex with $RuNH_2$ and possibly displace the phenanthroline or bipyridine ligands. Therefore, a variation on this thesis could involve the use of ruthenium terpyridine instead which is a much more stable

complex.

3,5-Dinitrobenzyl alcohol was found to be an efficient quencher with a quenching rate constant of $2.7 \times 10^9 \pm 2 \times 10^8$ $M^{-1}s^{-1}$ as well as a water-solubility of $5 \times 10^{-3}$ mol/L. Several synthetic routes were investigated as a means of generating 3,5-dinitrobenzylamine. The most efficient pathway seems to be via tritylamination of the commercially available 3,5-dinitrobenzyl chloride.

Several polymers were synthesized with apparent molecular weights of 400 000 g/mol or greater. A synthetic pathway allowing for covalent attachment of the dye and quencher to the polymer was determined and successfully accomplished. Consequently, through this study, it was demonstrated that the desired water-soluble polymer containing a water-soluble dye and quencher can be made.

Analysis of the luminescence decays of the RuNCS labelled polymers in DMF yielded three decay times of 20 ns, 170 ns, and 1000 ns with preexponential weights of 0.17, 0.11, and 0.72, respectively. The strongest contribution to the decay is that of 1000 ns which is characteristic of the dye. This demonstrates that PDMA can be labelled with a long-lived water-soluble dye. Furthermore, a luminescent decay of a polymer labelled with both RuNCS and DNB-$NH_2$ was measured and fit with a sum of three exponentials. The first two decay times of 3 ns and 10 ns occur on a very fast time scale and are too fast to be attributed to dynamic quenching. Therefore, static quenching is occurring although it is uncertain as to whether this static quenching is due to DNB-$NH_2$ or the 1-pyrenemethylamine contaminant. The third lifetime is 915 ns, similar to that of the unquenched dye.

Luminescence spectra of the PDMA samples were obtained and indicate that, upon introduction of the quencher onto the backbone, a complex is formed with the dye. This is evident by the broadening of the emission spectra for the polymer labelled with both the dye and quencher. This dye complex may be formed between either RuNCS and DNB-$NH_2$ or RuNCS and 1-pyrenemethylamine.

Continuation of this study requires additional synthesis of PDMA labelled with RuNCS and DNB-$NH_2$, ensuring that the labelled polymers do not contain pyrene contaminants, to repeat the luminescence experiments. If the same static quenching trends are observed, then it can be concluded that a complex is being formed between the DNB-$NH_2$ monomer and RuNCS rather than between 1-pyrenemethylamine and RuNCS. If this is in fact the case, DNB-OH could be reconsidered as the polymer quencher despite the consequent formation of an ester linkage.

The study of long range polymer chain dynamics with the FBM requires that 5-7 polymers be synthesized and labelled with the dye and varying amounts of quencher. The FBM can then be applied to these samples and the results will be compared to that of the pyrene labelled PDMA in DMF. Comparison of the two polymers will provide insight as to the versatility of the FBM since all the studies performed to date have used the chromophore pyrene.

Having prepared water-soluble polymers, the FBM can be applied to the polymer under aqueous conditions. This provides a starting point for several other interesting water-soluble systems. First of all, the chain dynamics of poly(N-isopropylacrylamide) (PNIPAM) in water can be studied. It is well known that PNIPAM undergoes a heat-induced coil-to-globule collapse in water at

32 $^{o}$C.[43] By labelling PNIPAM with a water soluble dye and quencher, and applying the FBM, the backbone dynamics of PNIPAM during this collapse can be studied. In addition, polypeptides can be labelled with the water-soluble dye and quencher. This study will provide information about protein folding.

# Appendix A

# Supporting Information for Dye and Quencher

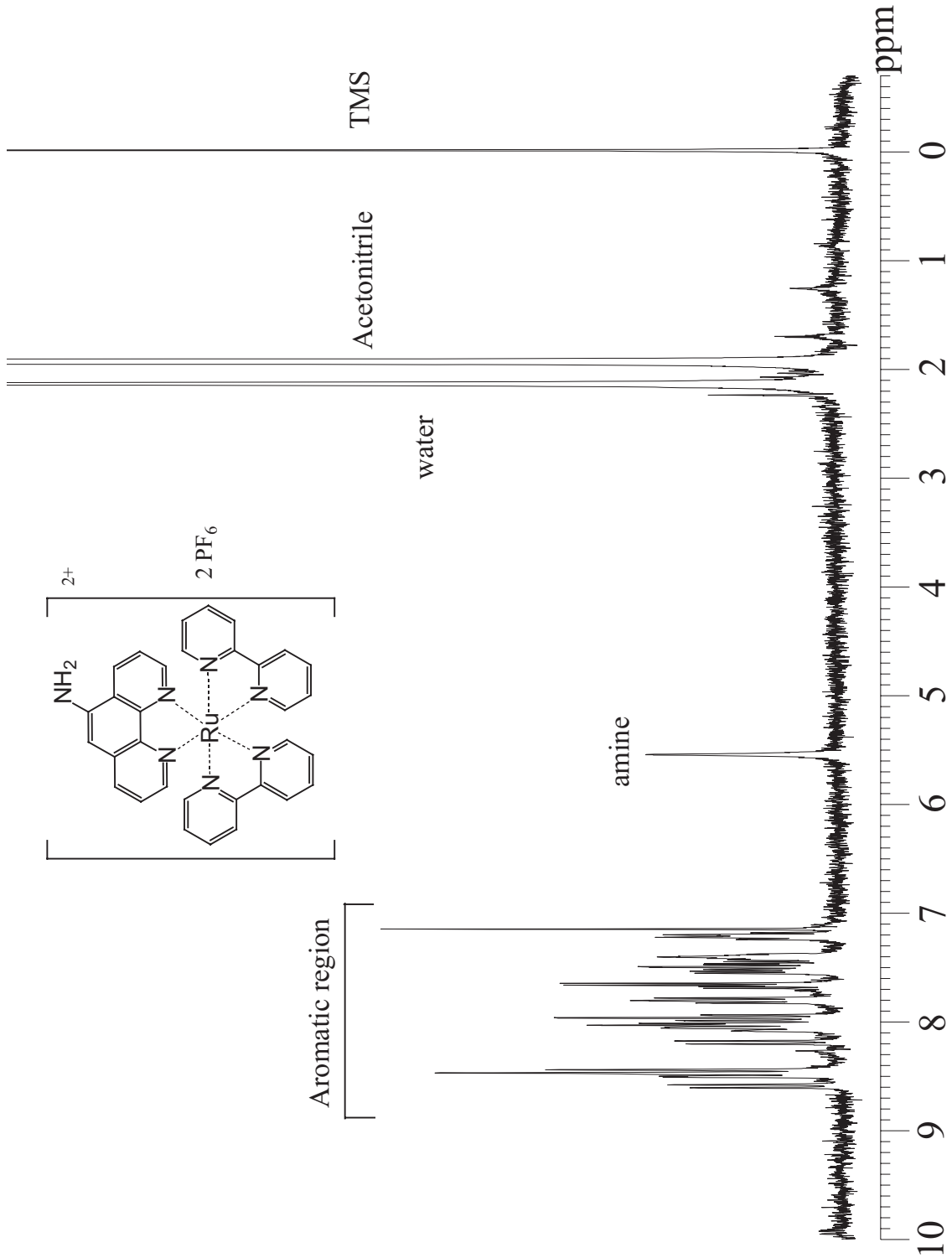


**FIGURE A.1** $^{1}$H NMR Spectrum of $RuNH_2$ in acetonitrile.

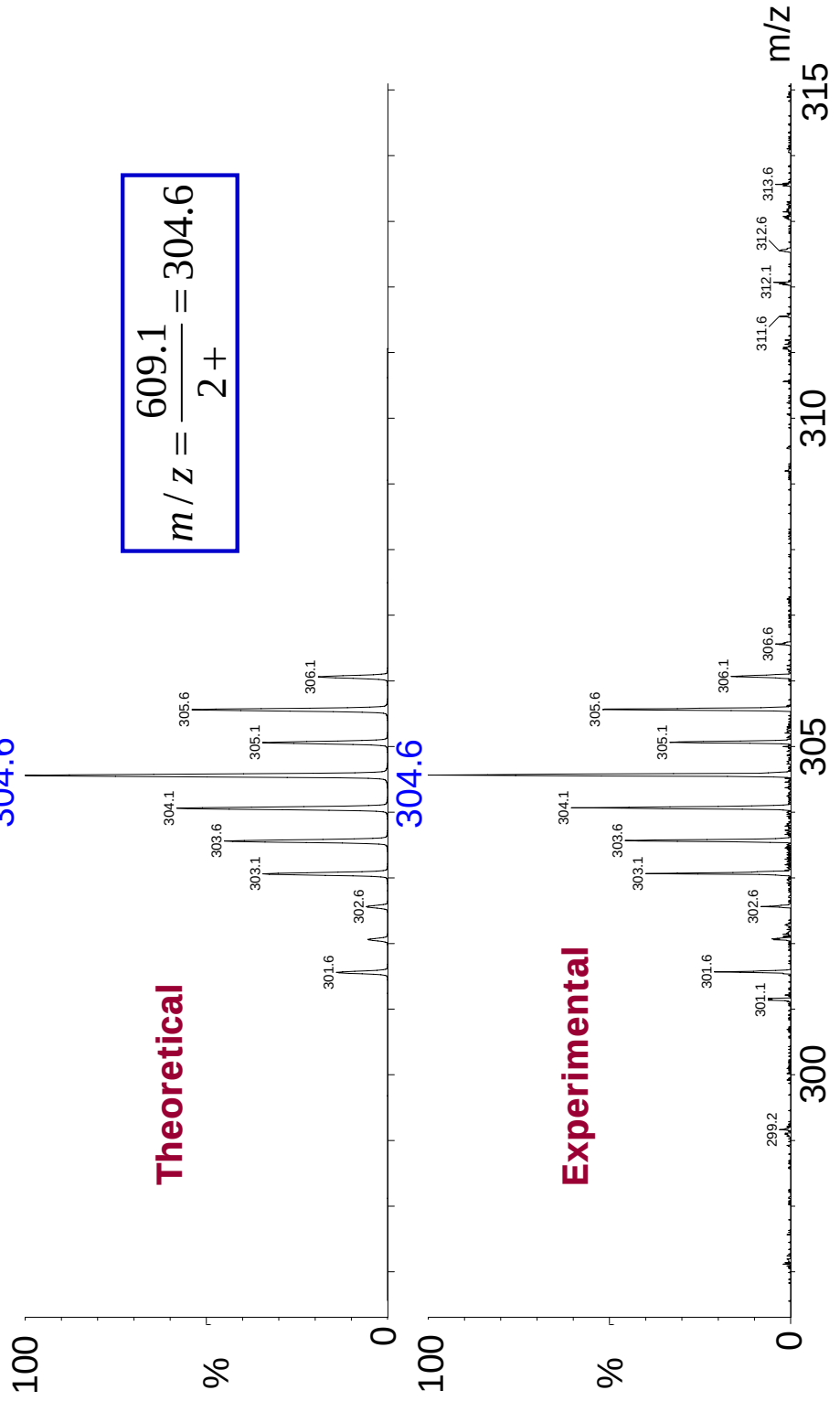


**FIGURE A.2** Mass spectrum of $RuNH_2$ in a 1:1 acetone:water mixture.

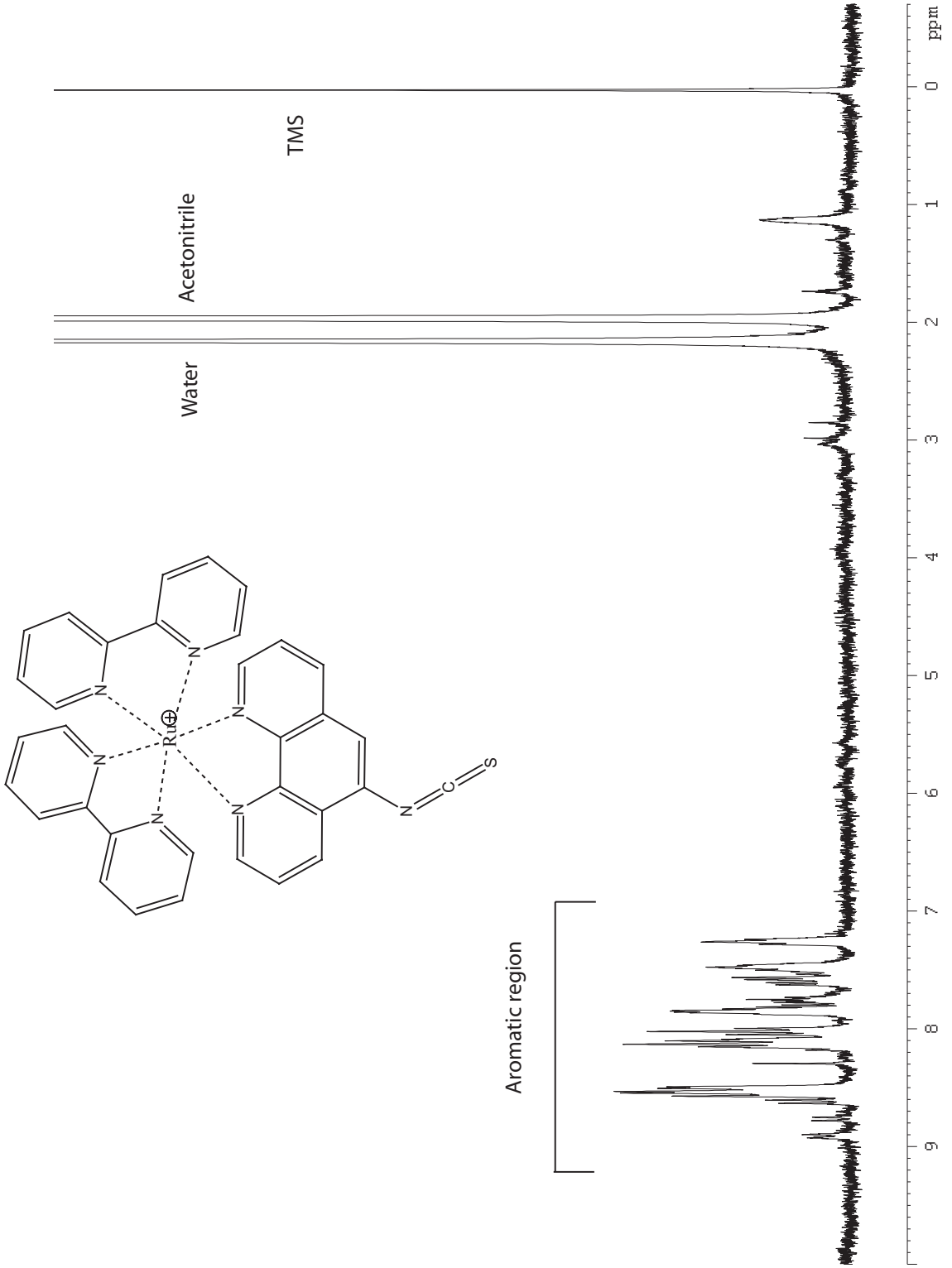


**FIGURE A.3** $^{1}$H NMR Spectrum of RuNCS in acetonitrile.

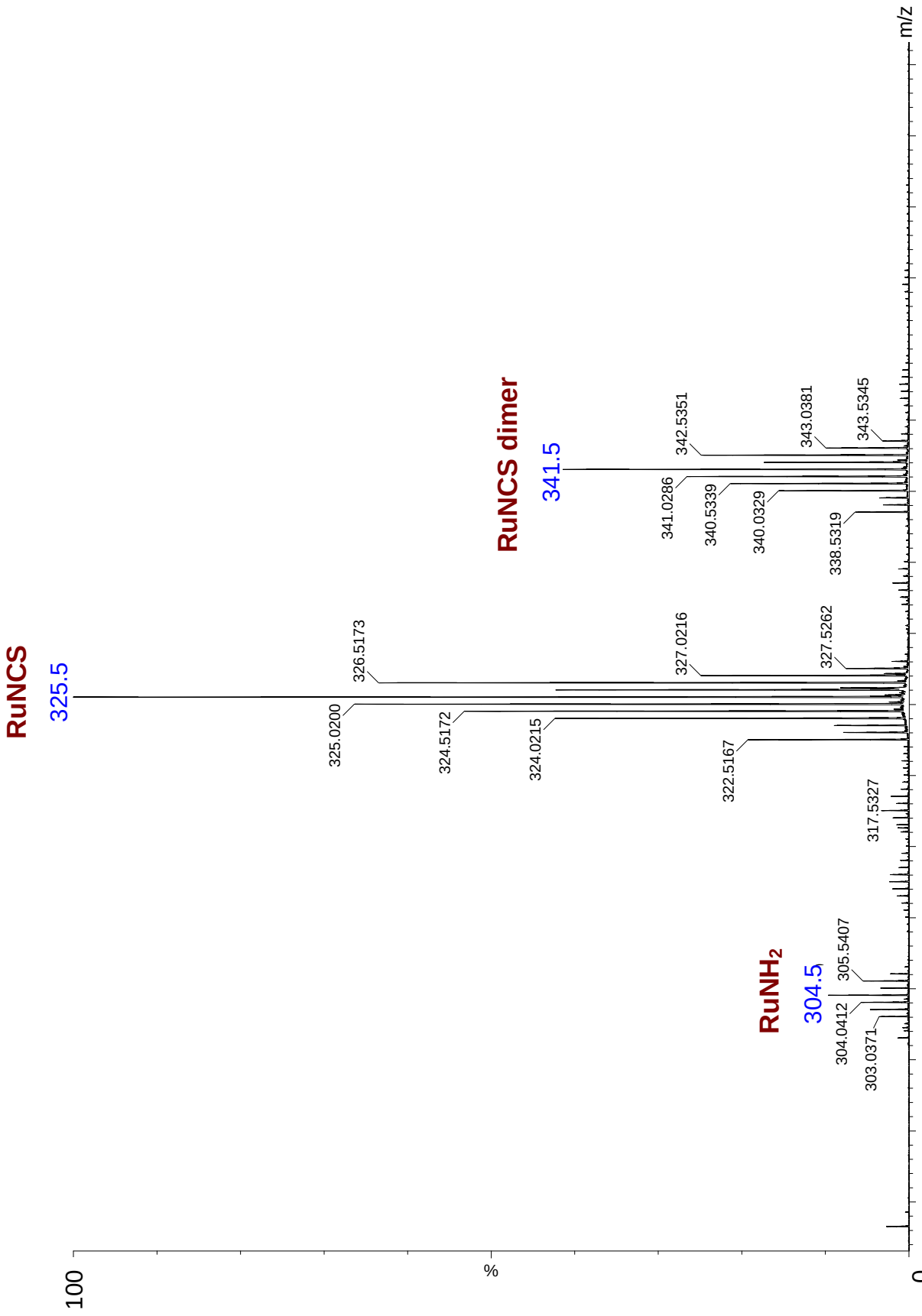


**FIGURE A.4** Mass spectrum of RuNCS in a 1:1 acetone:water mixture.

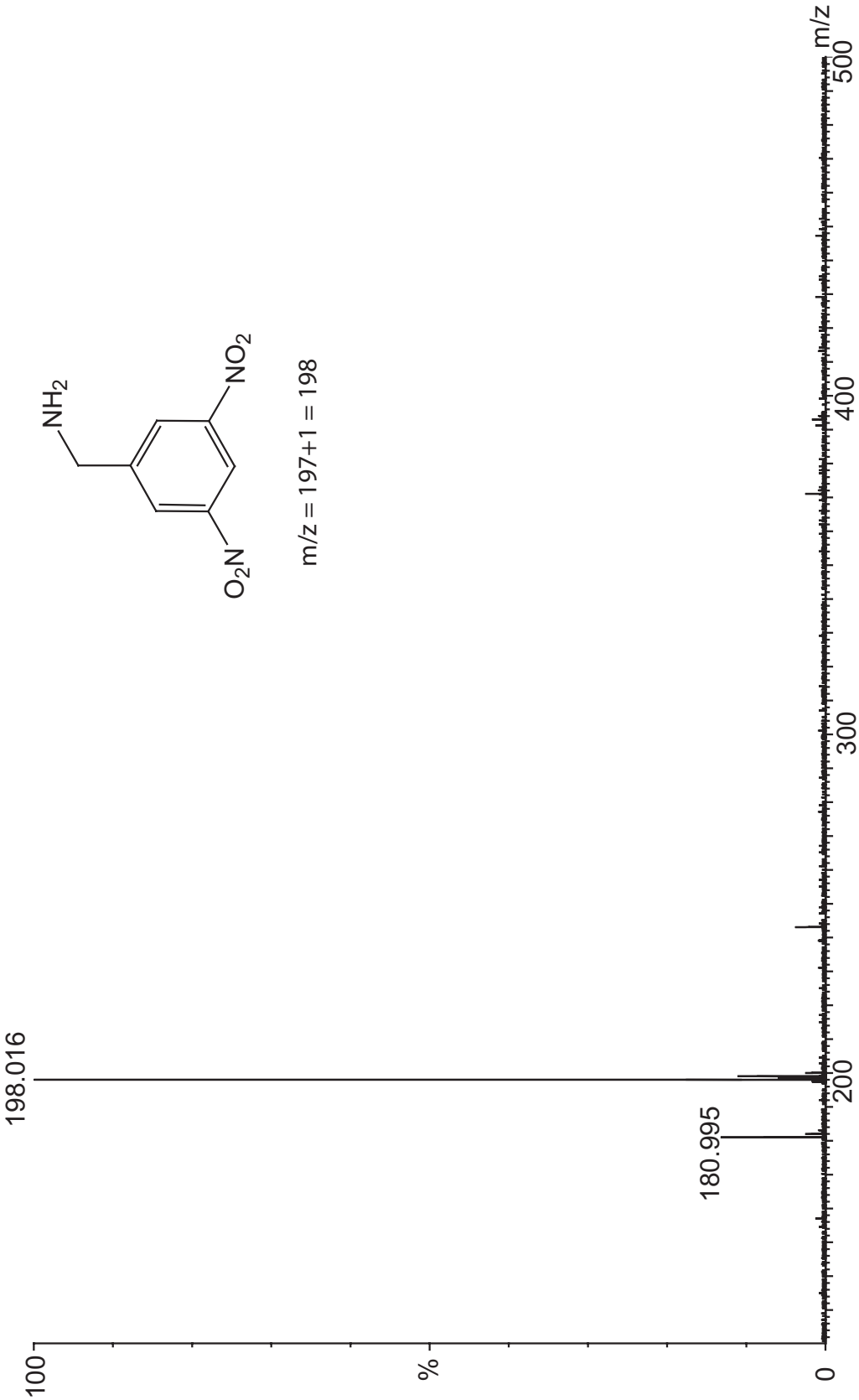


**FIGURE A.5** Mass spectrum of DNB-$NH_2$ in a 1:1 acetone:water mixture synthesized from DNB-Br. (MS/MS = 198)

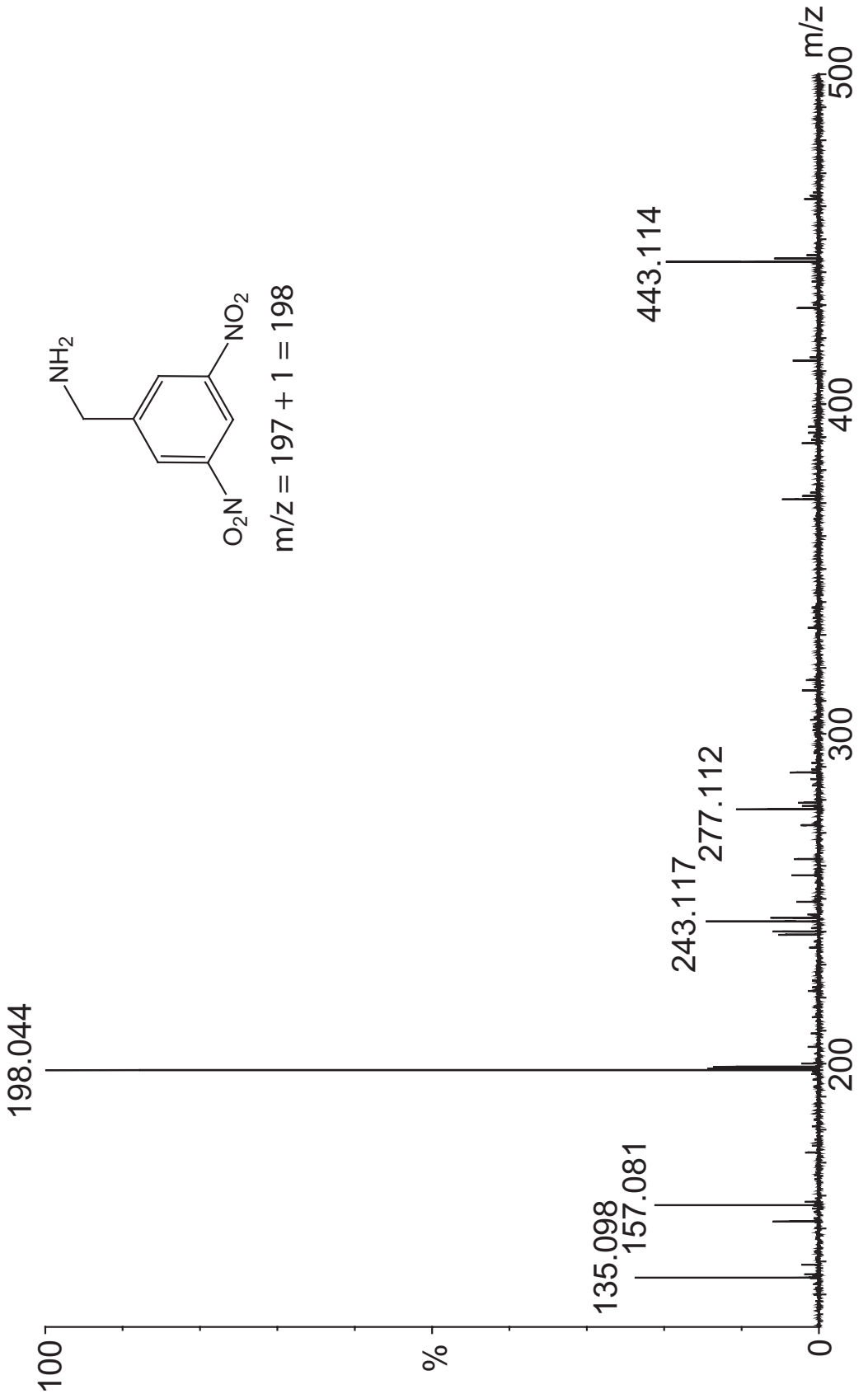


**FIGURE A.6** Mass spectrum of DNB-$NH_2$ in a 1:1 acetone:water mixture synthesized from DNB-Cl.

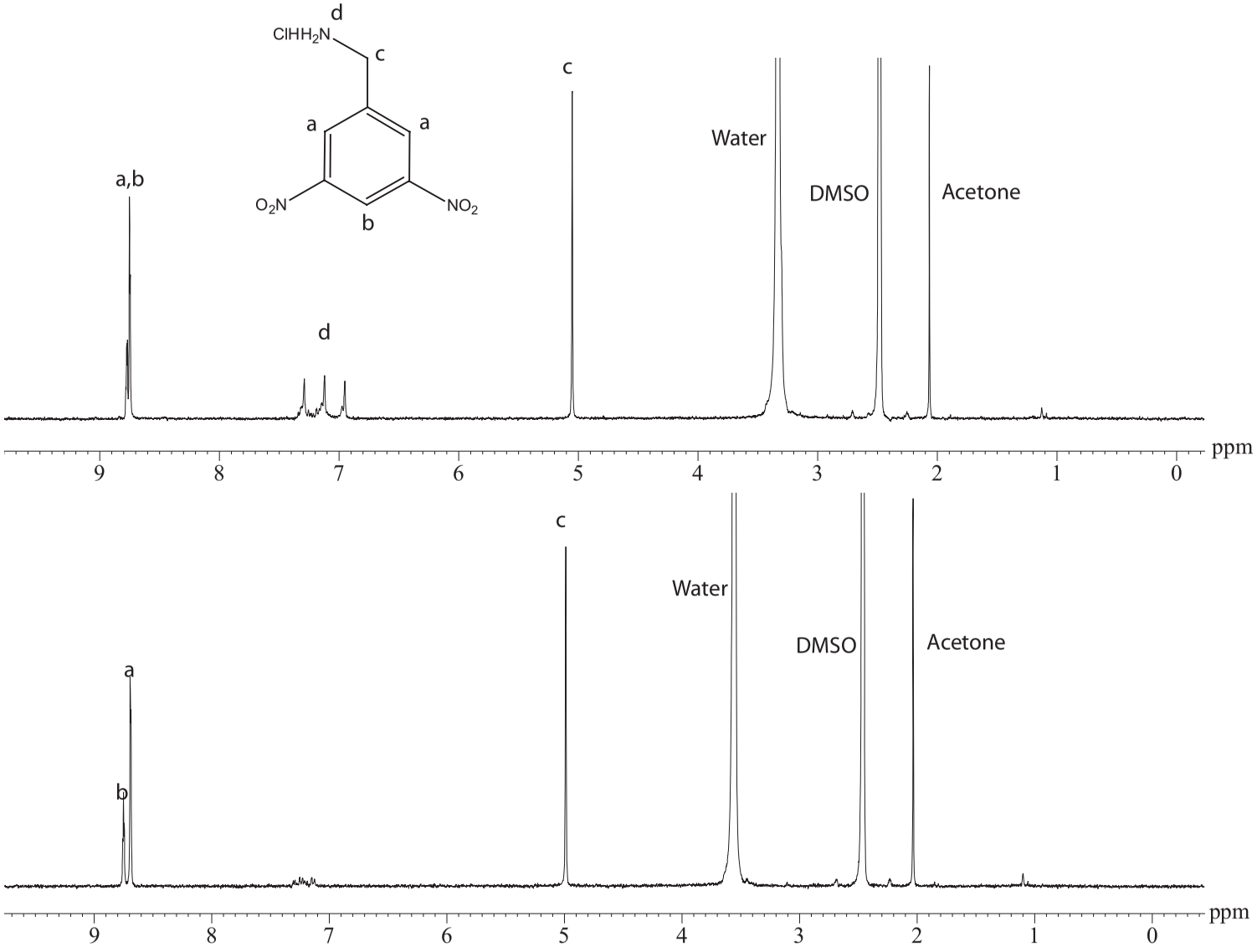


**FIGURE A.7** $^{1}$H NMR Spectrum of DNB-$NH_2$ in DMSO synthesized from DNB-Cl (**top**). $^{1}$H NMR Spectrum of DNB-$NH_2$ in DMSO synthesized from DNB-Cl with a small amount of $D_2O$ added (**bottom**).

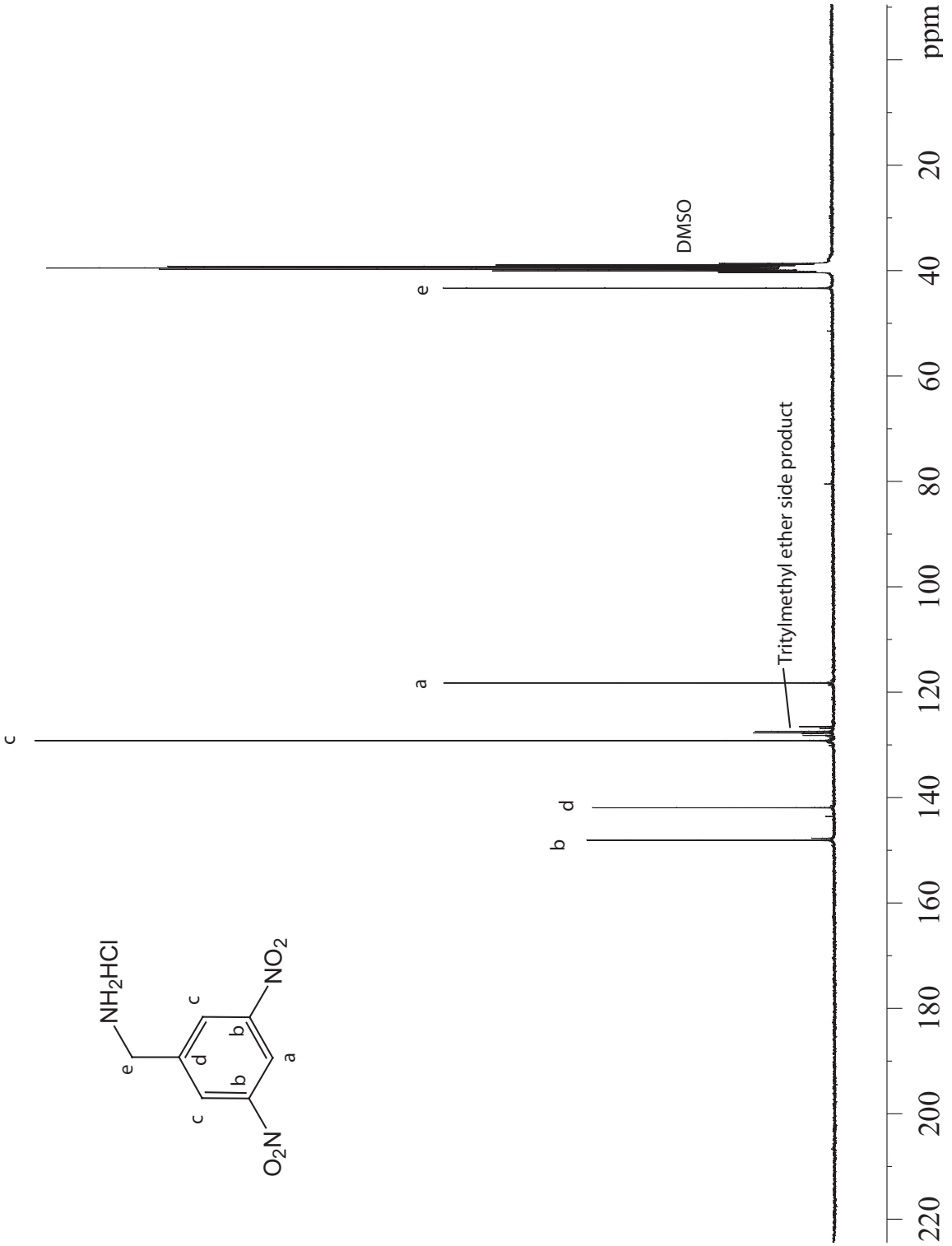


**FIGURE A.8** $^{13}C$ NMR Spectrum of DNB-$NH_2$ in DMSO synthesized from DNB-Cl.

# Appendix B

# NMR Spectra for Copolymerization

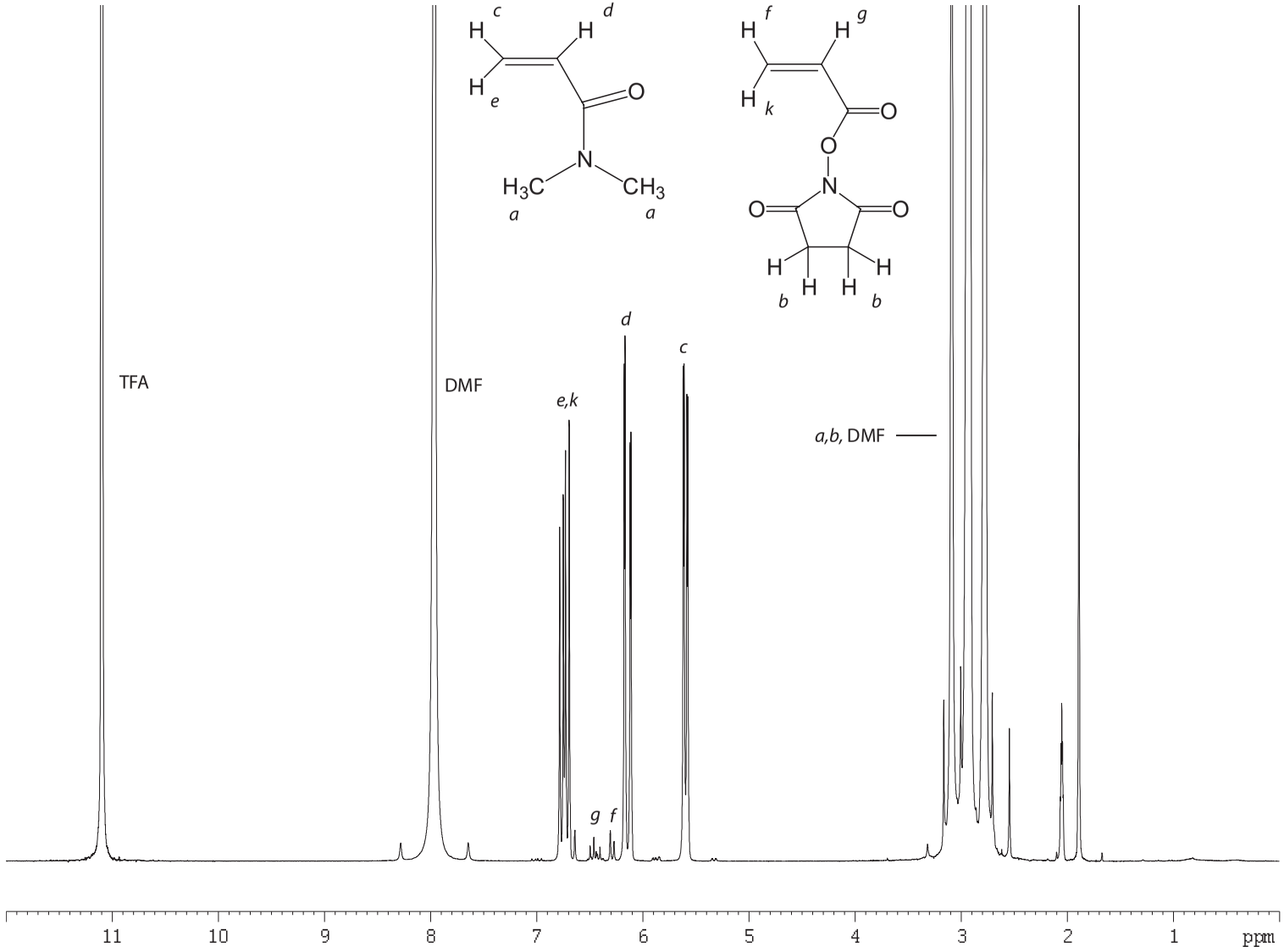


**FIGURE B.1** $^1$H NMR Spectrum of a copolymerization reaction mixture at $t = 0$. The NMR tube contains the TFA insert and the deuterated solvent is acetone.

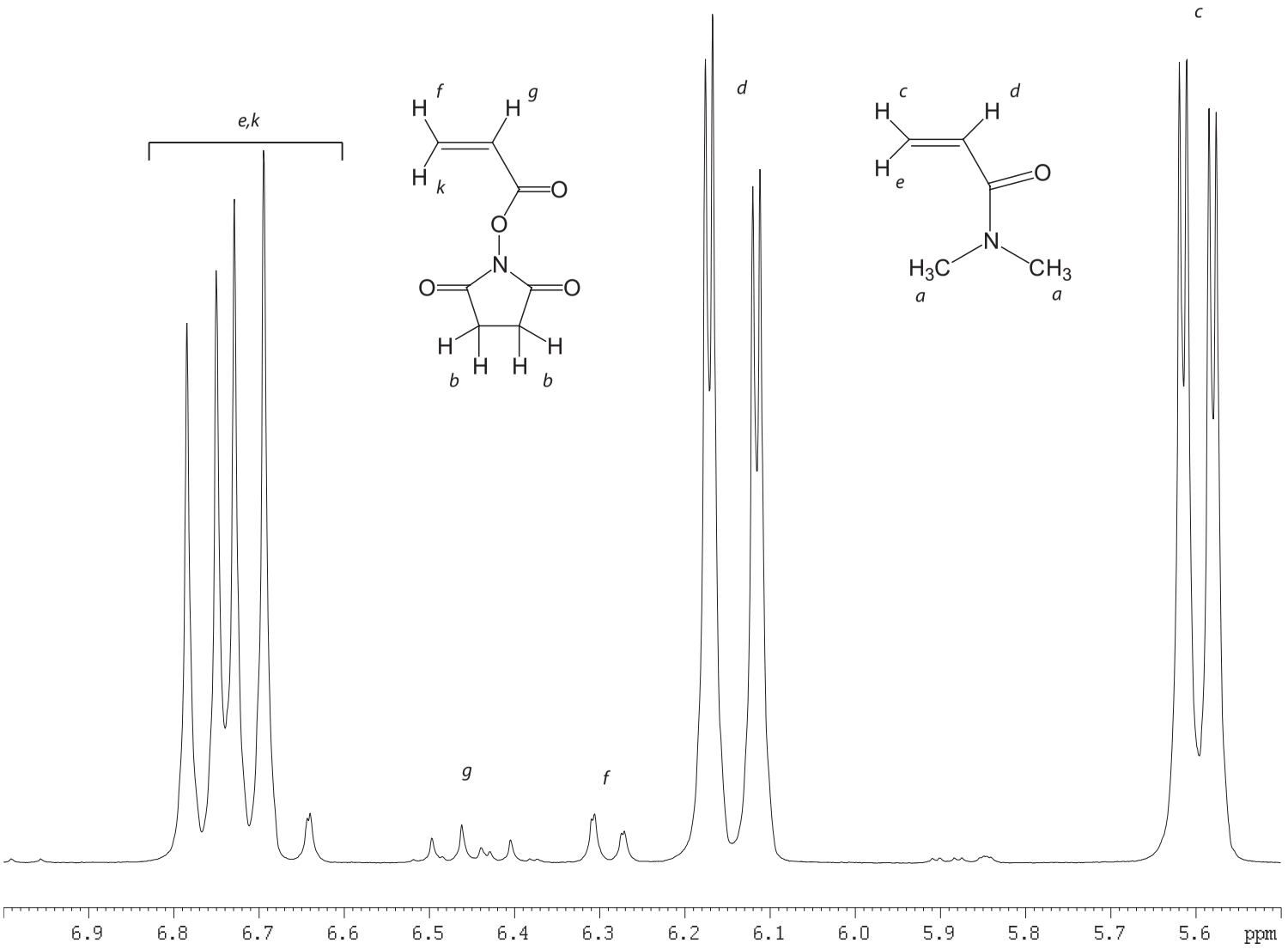


**FIGURE B.2** Enlarged alkene region of $^1$H NMR spectrum of the copolymerization reaction mixture at $t = 0$. Deuterated solvent is acetone.

# Appendix C

# Derivation of labelling equations

Derivation for Copolymer:

$M_x$ = mass of labelled monomer  Nx = number of labelled monomers

M = mass of unlabelled monomer  N = total number of monomers

x = fraction of labelled monomer  $\lambda$ = mol of labelled monomer/g polymer

$$\lambda = \frac{Nx}{NxM_x + N(1-x)M} \tag{C.1}$$

$$\lambda[xM_x + (1-x)M] = x \tag{C.2}$$

$$\lambda xM_x + \lambda M - \lambda Mx = x \tag{C.3}$$

$$x = [\lambda M_x - \lambda M - 1] = -\lambda M \tag{C.4}$$

$$x = \frac{\lambda M}{1 - \lambda(M_x - M)} \tag{C.5}$$

Derivation for Terpolymer:

| | |
|---|---|
| $\mathrm{M_q}$ = mass of quencher monomer | NQ = number of quencher monomers |
| $\mathrm{M_d}$ = mass of dye monomer | ND = number of dye monomers |
| M = mass of DMA monomer | N = total number of monomers |
| Q = fraction of quencher monomers | $\lambda_q$ = mol of quencher/g polymer |
| D = fraction of dye monomer | $\lambda_d$ = mol of dye/g polymer |

By definition

$$\lambda_d = \frac{D}{QM_q + DM_d + (1 - Q - D)M} \tag{C.6}$$

Rearranging this equation to isolate D and Q, we get

$$D = \lambda_d Q M_q + \lambda_d D M_d + \lambda_d M(1 - Q - D) \tag{C.7}$$

$$D(1 + M\lambda_d - M_d\lambda_d) + Q(M\lambda_d - M_q\lambda_d) = M\lambda_d \tag{C.8}$$

Similarly, for the quencher content, we have

$$\lambda_q = \frac{Q}{QM_q + DM_d + (1 - Q - D)M} \tag{C.9}$$

$$Q = \lambda_q QM_q + \lambda_q DM_d + \lambda_q M(1 - Q - D) \tag{C.10}$$

$$D(M\lambda_q - M_d\lambda_q) + Q(1 + M\lambda_q - M_q\lambda_q) = M\lambda_q \tag{C.11}$$

We now have 2 equations, Eqns. C.8, and C.11, and 2 unknowns, D and Q. By simplifying and rearranging them we obtain

$$D\frac{(1 + \lambda_d M - \lambda_d M_d)}{\lambda_d(M - M_q)} - \frac{\lambda_d M}{\lambda_d(M - M_q)} = D\frac{\lambda_q(M - M_d)}{1 + \lambda_q M - \lambda_q M_q)} - \frac{\lambda_q M}{1 + \lambda_q M - \lambda_q M_q)} \tag{C.12}$$

$$D\left[1 + \lambda_d M - \lambda_d M_d - \frac{\lambda_q(M - M_d)}{1 + \lambda_q M - \lambda_q M_q}\lambda_d(M - M_q)\right] = \lambda_d M - \frac{\lambda_q\lambda_d M(M - M_q)}{1 + \lambda_q M - \lambda_q M_q)} \tag{C.13}$$

$$
\begin{aligned}
D & \left[\frac{(1+\lambda_d M-\lambda_d M_d)(1+\lambda_q M-\lambda_q M_q)-\lambda_q\lambda_d(M-M_d)(M-M_q)}{1+\lambda_q M-\lambda_q M_q}\right] \\
= & \frac{\lambda_d M(1+\lambda_q M-\lambda_q M_q)-\lambda_q\lambda_d M(M-M_q)}{1+\lambda_q M-\lambda_q M_q} \qquad \text{(C.14)}
\end{aligned}
$$

$$
\begin{aligned}
D & [1+\lambda_d M-\lambda_d M_d+\lambda_q M+M\lambda_d M\lambda_q-\lambda_q\lambda_d M_d M \\
- & \lambda_q M_q-\lambda_q\lambda_d M_d M_q-\lambda_q\lambda_d(M-M_d)(M-M_q)] \\
= & \lambda_d M+\lambda_d M\lambda_q M-\lambda_d M\lambda_q M_q-\lambda_q\lambda_d M(M-M_q) \qquad \text{(C.15)}
\end{aligned}
$$

$$
\begin{aligned}
D & [1+\lambda_d(M-M_d)+\lambda_q(M-M_q)+\lambda_q\lambda_d(M-M_d)(M-M_q)-\lambda_q\lambda_d(M-M_d)(M-M_q)] \\
= & \lambda_d M+\lambda_d\lambda_q M(M-M_q)-\lambda_q\lambda_d M(M-M_q) \qquad \text{(C.16)}
\end{aligned}
$$

$$
D=\frac{\lambda_d M}{1+\lambda_q(M-M_q)+\lambda_d(M-M_d)} \qquad \text{(C.17)}
$$

$$
D=\frac{\lambda_d M}{1+\lambda_q M_q+\lambda_d M_d+M(\lambda_d+\lambda_q)} \qquad \text{(C.18)}
$$

# Appendix D

# References


[1] Miron, Y.; Morawetz, H. *Macromolecules* **1968**, *2*(2), 162–165.

[2] Tsunashima, Y. *J. Chem. Phys.* **1995**, *102*, 4673–4682.

[3] Polsona, J. M.; Gallant, J. P. *J. Chem. Phys.* **2006**, *124*, 184905.

[4] Morawetz, H. *J. Lumin.* **1989**, *43*, 59–71.

[5] Duhamel, J.; Pyrene Fluorescence to Study Polymeric Systems, *Molecular Interfacial phenomena of polymers and biopolymers*, Chen, P., Ed., Woodhead Publishing Limited, 2005; chapter 7, 214–248.

[6] Cunibertia, C.; Perico, A. *Euro. Polym. J.* **1977**, *13*, 369–374.

[7] Winnik, M. A.; Redpath, T.; Richards, D. H. *Macromolecules* **1980**, *13*, 328–335.

[8] Birks, J.; *Photophysics of Aromatic Molecules*, Wiley, 1970; chapter 7, 301–371.

[9] Mathew, A. K.; Siu, H.; Duhamel, J. *Macromolecules* **1999**, *32*, 7100–7108.

[10] Piçarra, S.; Duhamel, J.; Federov, A.; Martinho, J. *J. Phys. Chem. B* **2004**, *108*, 12009–12015.

[11] Kanagalingam, S.; Ngan, C. F.; Duhamel, J. *Macromolecules* **2002**, *35*, 8560–8570.

[12] Kanagalingam, S.; Spartalis, J.; Cao, T.-M.; Duhamel, J. *Macromolecules* **2002**, *35*, 8571–8577.

[13] Duhamel, J.; Sabesh Kanagalingam, T. J. O.; Ingratta, M. W. *J. Am. Chem. Soc.* **2003**, *125*, 12810–12822.

[14] Piçarra, S.; Relógio, P.; Afonso, C. A. M.; Martinho, J. M. G.; Farinha, J. P. S. *Macromolecules* **2003**, *36*, 8119–8129.

[15] Magde, D.; Wong, R.; Seybold, P. G. *Photochem. Photobiol.* **2002**, *75*, 327–334.

[16] Holmes, K. L.; Lantz, L. M.; *Methods in Cell Biology*, Academic Press, 2001; Vol. 63; chapter 9, 185–204.

[17] Wang, F.; Tan, W. B.; Zhang, Y.; Fan, X.; Wang, M. *Nanotechnology* **2006**, *17*, R1–R13.

[18] Juris, A.; Balzani, V.; Barigelletti, F.; Campagna, S.; Belser, P.; Zelewsky, A. V. *Coord. Chem. Rev.* **1988**, *84*, 85–277.

[19] Friedman, A.; Chambron, J.; Sauvage, J.; Turro, N.; Barton, J. *J. Am. Chem. Soc.* **1990**, *112*, 4960–4962.

[20] Ruba, E.; Hart, J.; Barton, J. *Inorg. Chem.* **2004**, *13*, 4570–4578.

[21] Walsh, M.; Ryan, E.; O'Kennedy, R.; Vos, G. *J. Inorganic Biochem.* **1996**, *63*, 215–221.

[22] Terpetsching, E.; Szmacinski, H.; Malak, H.; Lakowicz, J. R. *Biophys. J.* **1995**, *68*, 342–350.

[23] Rudmann, H.; Shimada, S.; Rubner, M. *J. Am. Chem. Soc.* **2002**, *124*, 4918–4921.

[24] Medlycott, E.; Hanan, G. *Chem. Soc. Rev.* **2005**, *34*, 133–142.

[25] Carraway, E.; Demas, J.; DeGraff, B.; Bacon, J. *Anal. Chem.* **1991**, *63*, 337–342.

[26] Lakowicz, J. R.; *Principles of Fluorescence Spectroscopy*, Kluwer Academic/Plenum Publishers, 1999; 2nd ed.

[27] Ellis, C.; Margerum, L.; Murray, R.; Meyer, T. *Inorg. Chem.* **1983**, *22*, 1283–1291.

[28] Ryan, E. M.; O'Kennedy, R.; Feeney, M. M.; Kelly, J. M.; Vos, J. G. *Bioconjugate Chem.* **1992**, *3*, 285–290.

[29] Glazier, S.; Barron, J. A.; Morales, N.; Ruschak, A. M.; Houston, P. L.; Abruña, H. D. *Macromolecules* **2003**, *36*, 1272–1278.

[30] May, W. E.; Wasik, S. P.; Freeman, D. H. *Anal. Chem.* **1978**, *50*, 997–1000.

[31] Caspar, J. V.; Meyer, T. J. *J. Am. Chem. Soc.* **1983**, *105*, 5583–5590.

[32] Lakowicz, J. R.; *Principles of Fluorescence Spectroscopy*, Kluwer Academic/Plenum Publishers, 1999; 255; 2nd ed.

[33] Barrett, A. G.; Braddock, D. C.; McKinnell, R.; Waller, F. J. *Synlett* **1999**, (9), 1489–1490.

[34] Williams, R. M.; Ehrlich, P. P.; Zhai, W.; Hendrix, J. *J. Org. Chem.* **1987**, *52*, 2615–2617.

[35] Theodorou, V.; Raoussis, V.; Strongilos, A.; Zelepos, E.; Eleftheriou, A.; Dimitriou, M. *Tett. Lett.* **2005**, *46*, 1357–1360.

[36] Wiley, G. A.; Hershkowitz, R. L.; Rein, B. M.; Chung, B. C. *J. Am. Chem. Soc.* **1964**, *86*, 964–965.

[37] Du, M.; Ge, X.-J.; Liu, H.; Bu, X.-H. *J. Mol. Struct.* **2002**, *610*, 207–213.

[38] Vrcelj, R. M.; Sherwood, J. N.; Kennedy, A. R.; Gallagher, H. G.; Gelbrich, T. *Cryst. Growth Des.* **2003**, *3*, 1072–1032.

[39] Robertson, J. M.; White, J. G. *J. Chem. Soc.* **1947**, 358–68.

[40] Berlman, I. B.; *Handbook of fluorescence spectra of aromatic molecules*, Academic Press, 1971.

[41] Relógio, P.; Chareyre, M.-T.; Farinha, J. P. S.; Martinho, J. M. G.; Pichot, C. *Polymer* **2004**, *45*, 8639–8649.

[42] Odian, G.; *Principles of Polymerization*, John Wiley Sons, Inc., 1991; chapter 6, 464; 3rd ed.

[43] Heskins, M.; E.Guillet, J. *Macromol. Sci. Chem. A2* **1968**, 1441.